INTERNATIONAL STANDARD

ISO 11221

First edition
2011-08-01

Space systems — Space solar panels — Spacecraft charging induced electrostatic discharge test methods

Systèmes spatiaux — Panneaux solaires spatiaux — Matériaux d'essai de décharge électrostatique induite par la charge du vaisseau spatial

Reference number
ISO 11221:2011(E)

COPYRIGHT PROTECTED DOCUMENT

ISO copyright office
Case postale 56 • CH-1211 Geneva 20
Tel. + 41 22 749 01 11
Fax + 41 22 749 09 47
E-mail copyright@iso.org
Web www.iso.org

Published in Switzerland

Contents

Page

Foreword

ISO (the International Organization for Standardization) is a worldwide federation of national standards bodies (ISO member bodies). The work of preparing International Standards is normally carried out through ISO technical committees. Each member body interested in a subject for which a technical committee has been established has the right to be represented on that committee. International organizations, governmental and non-governmental, in liaison with ISO, also take part in the work. ISO collaborates closely with the International Electrotechnical Commission (IEC) on all matters of electrotechnical standardization.

International Standards are drafted in accordance with the rules given in the ISO/IEC Directives, Part 2.

The main task of technical committees is to prepare International Standards. Draft International Standards adopted by the technical committees are circulated to the member bodies for voting. Publication as an International Standard requires approval by at least 75 % of the member bodies casting a vote.

Attention is drawn to the possibility that some of the elements of this document may be the subject of patent rights. ISO shall not be held responsible for identifying any or all such patent rights.

ISO 11221 was prepared by Technical Committee ISO/TC 20, *Aircraft and space vehicles*, Subcommittee SC 14, *Space systems and operations*.

Space systems — Space solar panels — Spacecraft charging induced electrostatic discharge test methods

1 Scope

This International Standard specifies qualification and characterization test methods to simulate plasma interactions and electrostatic discharges on solar array panels in space. This International Standard is applicable to solar array panels made of crystalline silicon, gallium arsenide (GaAs) or multi-junction solar cells. This International Standard addresses only surface discharges on solar panels.

2 Terms and definitions

For the purposes of this document, the following terms and definitions apply.

2.1
active gap
gap between solar cells across which a potential difference is present when the solar array power is available

2.2
blow-off
emission of negative charges into space due to an electrostatic discharge

2.3
collisionless plasma
plasma in which the mean free paths of electron-neutral, ion-neutral and coulomb collisions are longer than the scale length of interest

NOTE Chamber length is an example of a scale length of interest.

2.4
differential charging
spacecraft charging where any two points are charged to different potentials

2.5
differential capacitance
capacitance between any two points in a spacecraft, especially between the insulator surface and the spacecraft body

2.6
differential voltage
potential difference between any two points in a spacecraft during spacecraft charging, especially between the insulator exterior surface potential and the spacecraft chassis potential

2.7
discharge inception voltage
lowest voltage at which discharges of specified magnitude will recur when a DC voltage is applied between any two points in a spacecraft, especially between the insulator surface and the spacecraft body

2.8
electrical breakdown
failure of the insulation properties of a dielectric, resulting in a sudden release of charge with possible damage to the dielectric concerned

2.9
electric propulsion
spacecraft propulsion system in which the thrust is generated by accelerating charged particles that are neutralized before they are ejected in order to produce a jet

2.10
electrostatic discharge
electrical breakdown of dielectric or gas or vacuum gaps, and also of surface interface of dissimilar materials, caused by differential charging of parts of dielectric materials and their interfaces

2.11
gap distance
distance between biased cells or conductors

2.12
glow discharge
gaseous discharge with a surface glow near the cathode surface

NOTE The origin of the ionized gas is mostly ambient neutral gas molecules rather than metal vapour from the cathode surface.

2.13
inverted potential gradient
inverted voltage gradient
result of differential charging where the insulating surface or dielectric reaches a positive potential with respect to the neighbouring conducting surface or metal

NOTE This phenomenon is also known as PDNM (positive dielectric negative metal).

2.14
non-sustained arc
passage of current from an external source through a conductive path that lasts only while the primary discharge current flows

See Figure 1.

2.15
normal potential gradient
normal voltage gradient
result of differential charging where the insulating surface or dielectric reaches a negative potential with respect to the neighbouring conducting surface or metal

NOTE This phenomenon is also known as NDPM (negative dielectric positive metal).

2.16
permanent sustained arc
passage of current from an external source through a conductive path that keeps flowing until the external source is intentionally shut down

See Figure 1.

NOTE Some permanent sustained arcs may leave a permanent conductive path even after the shut-down.

2.17
Poisson process
stochastic process in which events occur independently of one another

2.18
power generation voltage
potential difference between the positive and negative terminals of a solar array string

2.19
primary arc
trigger arc
developed phase of a primary discharge, under an inverted potential gradient, which is associated with cathodic spot formation at a metallic or semiconductor surface

2.20
primary discharge
initial electrostatic discharge which, by creating a conductive path, can trigger a secondary arc

See Figure 1.

NOTE The current can include blow-off current and surface flashover current.

2.21
punch-through
dielectric breakdown between two sides of an insulator material

2.22
ram
space in front of and adjacent to a spacecraft in which the plasma density can be enhanced by the motion of the spacecraft

2.23
satellite capacitance
absolute capacitance
capacitance between a satellite body and the ambient plasma

2.24
secondary arc
passage of current from an external source, such as a solar array, through a conductive path initially generated by a primary discharge

NOTE Figure 1 shows the various stages of a secondary arc.

2.25
snapover
phenomenon caused by secondary electron emission that can lead to electron collection on insulating surfaces in an electric field

2.26
solar array front surface
solar array surface where solar cells are laid down

NOTE Solar cells are laid down on the side of a solar panel that normally faces the sun.

2.27
solar array back surface
solar array surface where solar cells are not laid down

NOTE Solar cells are not laid down on the side of a solar panel that normally faces away from the sun.

2.28
surface charging
deposition of electrical charges onto, or their removal from, external surfaces

2.29
surface flashover
surface discharge propagating laterally over a dielectric material

NOTE Surface flashover is sometimes called a “brushfire discharge”.

2.30
temporary sustained arc
passage of current from an external source through a conductive path that lasts longer than a primary discharge current pulse but terminates without leaving a permanent conductive path

See Figure 1.

2.31
wake
trail of rarefied plasma left behind by a moving spacecraft

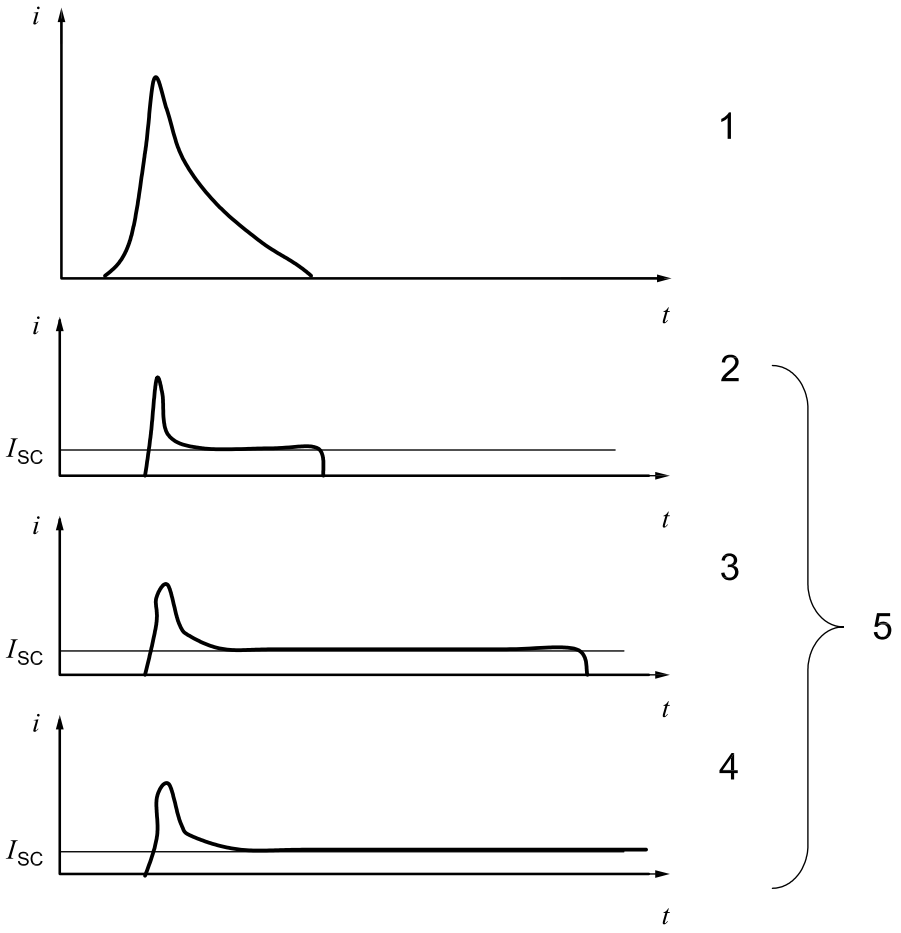

Key
1 primary discharge (blow-off + flashover)
2 non-sustained arc (NSA)
3 temporary sustained arc (TSA)
4 permanent sustained arc (PSA)
5 secondary arc

i current
I_{SC} short-circuit current of one or more solar array circuits
t time

The primary discharge is fed by absolute and differential capacitances. The secondary arc is fed by the solar array power.

Figure 1 — Stages of secondary arc

3 Symbols and abbreviated terms

3.1 Symbols

A_s area of surface of plasma

C_{BC} bypass capacitance

C_{CG} differential capacitance

C_{GS} capacitor representing capacitance between solar panel structure and ambient plasma

C_{kapton} capacitor representing capacitance underneath the cells through the Kapton layer

C_{sat} satellite capacitance

C_{string} capacitor representing capacitance of solar array string

C_v capacitance per unit area of coverglass

C_1 capacitor representing capacitance of solar array string and capacitance underneath the cells through the Kapton layer

C_2 capacitor representing capacitance of solar array string and capacitance underneath the cells through the Kapton layer

C_3 capacitor representing capacitance of solar array string and capacitance underneath the cells through the Kapton layer

D_1 fast switching diode

D_2 fast switching diode

D_3 fast switching diode

d_{sh} sheath thickness

I_0 reverse saturation-current density, in amperes per square metre (A/m^2)

I_1 power supply representing power generated by the solar array

I_{sc} short-circuit current of one or more solar array circuits

$I_{section}$ current of a solar array section

I_{string} current of a solar array string

i current

j number of bins

k Boltzmann constant

L_{ext} inductance to form the pulse current shape

n diode constant

P_i probability that an event occurs in the i-th bin

Q charge

q elementary charge

R resistance

R_{ext} resistance to form the pulse current shape

R_L resistance to adjust the voltage between two strings under test

$R_{section}$ $U_{section}/I_{section}$ resistance needed to get the right voltage and current in the loop simulating the solar panels section

R_{string} U_{string}/I_{string} resistance needed to get the right voltage and current across the solar cells simulating the solar array string under arcing test

r radius of plasma

T temperature, in kelvins (K)

T_e electron temperature

T_i ion temperature

t time

t_{ESD} time to threshold differential voltage

U_1 constant current source

U_2 constant voltage source

$U_{section}$ voltage of a solar array section

U_{string} voltage of a solar array string

V_b power supply representing charging potential of spacecraft body

v_p velocity of plasma wavefront

ΔV potential difference

θ angle

λ_D Debye length

ρ_e electron density

ρ_i ion density

ϕ_{CG} coverglass potential

ϕ_{sat} satellite body potential

3.2 Abbreviated terms

eV electron volt (1 eV = 1,602 × 10^{-19} J)

CIC coverglass interconnect cell

ESD electrostatic discharge

GEO geosynchronous orbit

IPG inverted potential gradient

LEO low Earth orbit

NPG normal potential gradient

NSA non-sustained arc

PA primary arc

PEO polar Earth orbit

PI plasma interaction

PSA permanent sustained arc

TSA temporary sustained arc

4 Tailoring

Specifications described in this International Standard are tailorable upon agreement between the customer and the supplier.

5 Test items

NOTE Annex A provides an overview of the subject of spacecraft charging and electrostatic discharge (ESD) phenomena for readers who are not familiar with the subject.

The aims of the plasma interaction (PI) and ESD tests are to simulate the detrimental phenomena anticipated in space for a given solar array design, to evaluate a design's resistance to the phenomena and to provide data necessary for the judgment of qualification and characterization.

Figures 2 and 3 present the test items specified in this International Standard, with flow charts to summarize the logic flow of each test. The purpose of a preliminary test for ESD statistics is to define the statistics helpful for selecting the test parameters (such as the number of primary discharges inflicted upon a test coupon), defining the margins of the test parameters and defining the confidence level of the test results. If proper statistics for these numbers and probabilities are already available, the preliminary test is not required for the qualification of secondary arcs. Annex B provides a brief rationale of the structure of the flow chart in Figure 2.

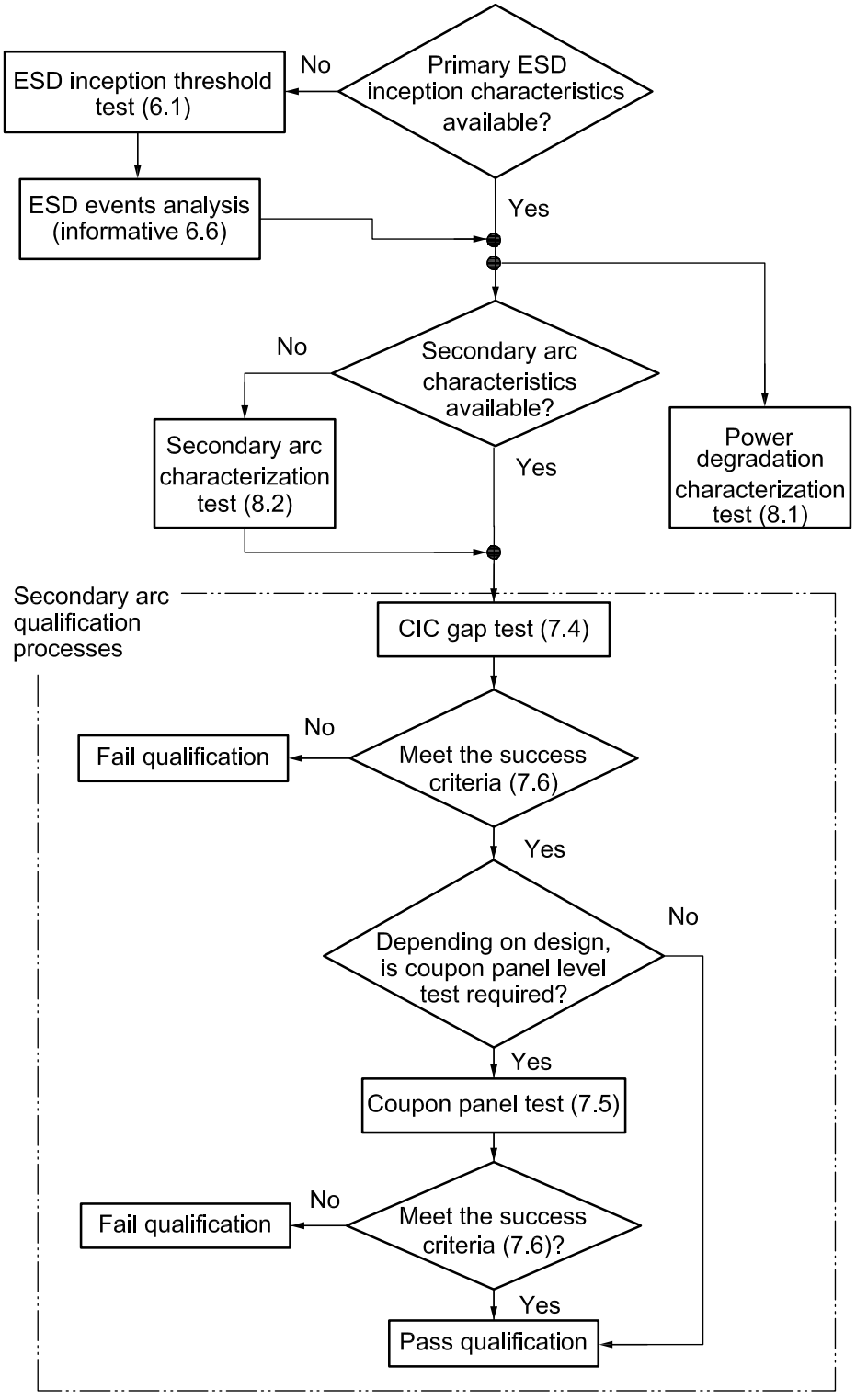

Figure 2 — Logic flow of ESD tests

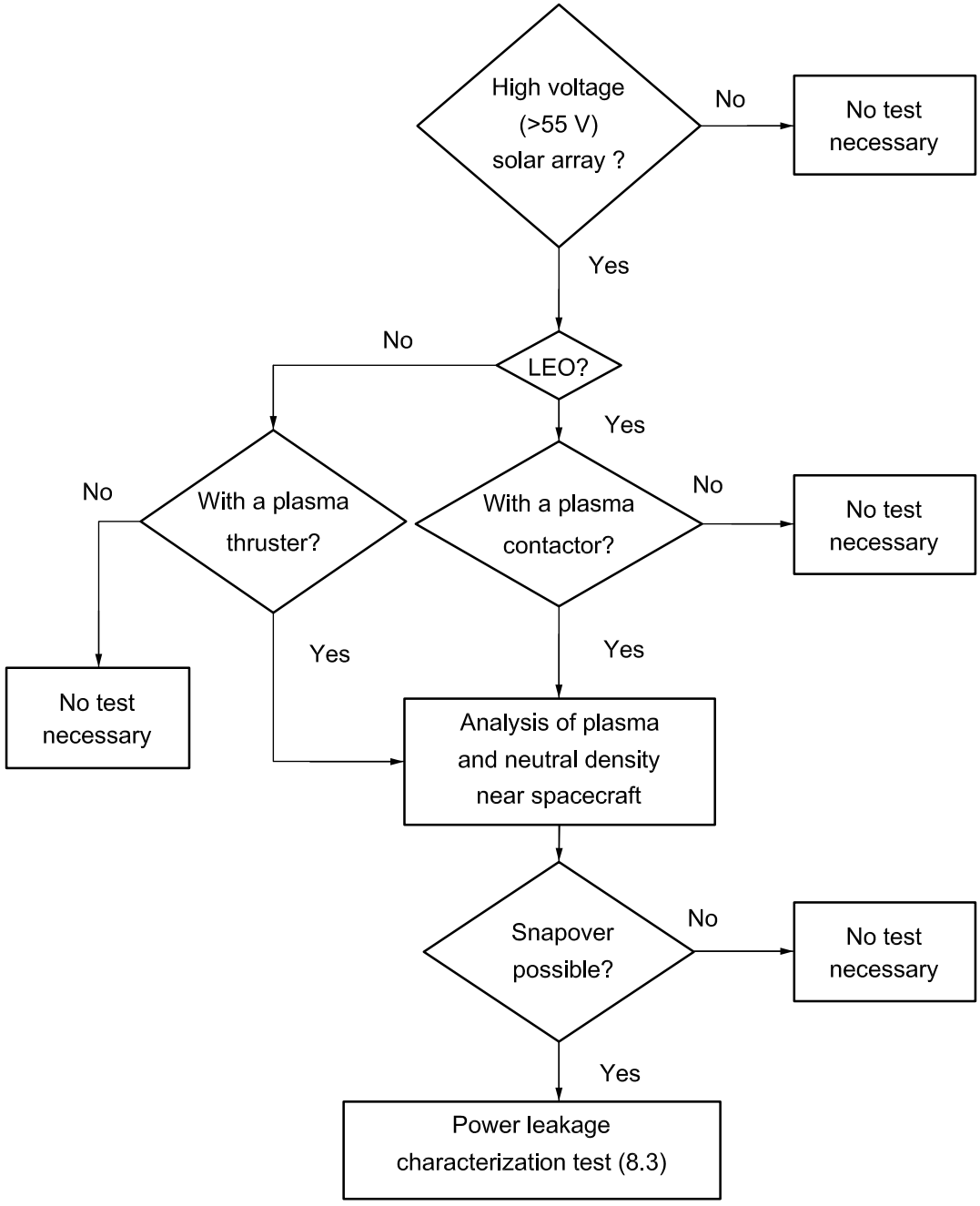

Figure 3 — Logic flow for determining the necessity of a power leakage characterization test

6 Preliminary tests for ESD inception statistics

6.1 Purpose

The purpose of this test is to characterize the ESD (primary discharge) inception threshold in terms of differential voltage between the coverglasses and the solar array circuit. This differential voltage can be used as a tool to estimate the number of ESD events during the mission lifetime in orbit.

6.2 Test facility

The test facility shall be able to simulate the charging processes of a solar array insulator in orbit. If the solar array is for a GEO satellite, the solar array insulator shall be charged using either an energetic electron beam or UV irradiation, or a combination of both, in a vacuum chamber with a pressure lower than 1×10^{-3} Pa ($7{,}5 \times 10^{-6}$ Torr). The electron energy shall be less than 30 keV so that the charging takes place mostly over the insulator surface, and not below it. The vacuum chamber for a geosynchronous orbit (GEO) solar array test shall be equipped with an adequate device to determine the insulator charging potential, such as a non-contacting surface potential probe, preferably mounted on an (x)-(y) scanning device.

If the solar array is for a low Earth orbit (LEO) spacecraft, the solar array insulator shall be charged by a low-energy plasma with a temperature below 10 eV in a vacuum chamber with a pressure that guarantees a collisionless plasma. If the solar array is for a polar Earth orbit (PEO) spacecraft and auroral electrons are responsible for differential charging, the solar array insulator should be charged using an energetic electron beam. If the solar array is for a PEO spacecraft and low-energy ionospheric ions are responsible for differential charging, the solar array insulator should be charged using a low-energy plasma. See Annex C for the minimum chamber size for a low-energy plasma test.

The test facility shall be equipped with a device to record an adequate image of the test coupon during the test so that ESD locations can be identified either during or after the test.

6.3 Test coupon

The test coupon(s) shall consist of at least three strings of three cells to represent a cell surrounded by other cells. The test coupon(s) should

a) reflect the production variation with respect to parameters that can affect the ESD inception threshold, such as degree of grouting, coverglass overhang, cell spacing, etc. on the total number of cells on the test coupon(s),

b) include all the features of a flight panel, such as bus bars, through-holes, terminal strips, wire harness, hold-down, etc.,

c) include the mitigation techniques that represent the flight model as closely as possible, if the solar panel design involves ESD mitigation techniques such as a dissipative coating, and

d) consider the worst condition during the life of the spacecraft, such as after thermal cycling, repaired cells, and other conditions that can lead to a greater risk of ESD and secondary arcs.

6.4 External circuit

In the test, the vacuum chamber serves as the circuit ground. If the charging situation in space is the inverted potential gradient, bias the test coupon to a negative potential with a DC power supply. If the charging situation is the normal potential gradient, ground the test coupon. (See Figure 4 for a circuit diagram.) A small amount of capacitance may be connected to the DC power supply if a brighter flash of ESD light is needed to identify its location. Limit the capacitance so that the electrostatic energy dissipated does not cause degradation of the solar cells on the test coupon(s). An energy of less than 5 mJ is recommended. As the capacitance of a coupon alone sometimes exceeds the limit, external capacitance should not be used for a large coupon of more than about 20 cells. To record the ESD in this event, use a sensitive camera.

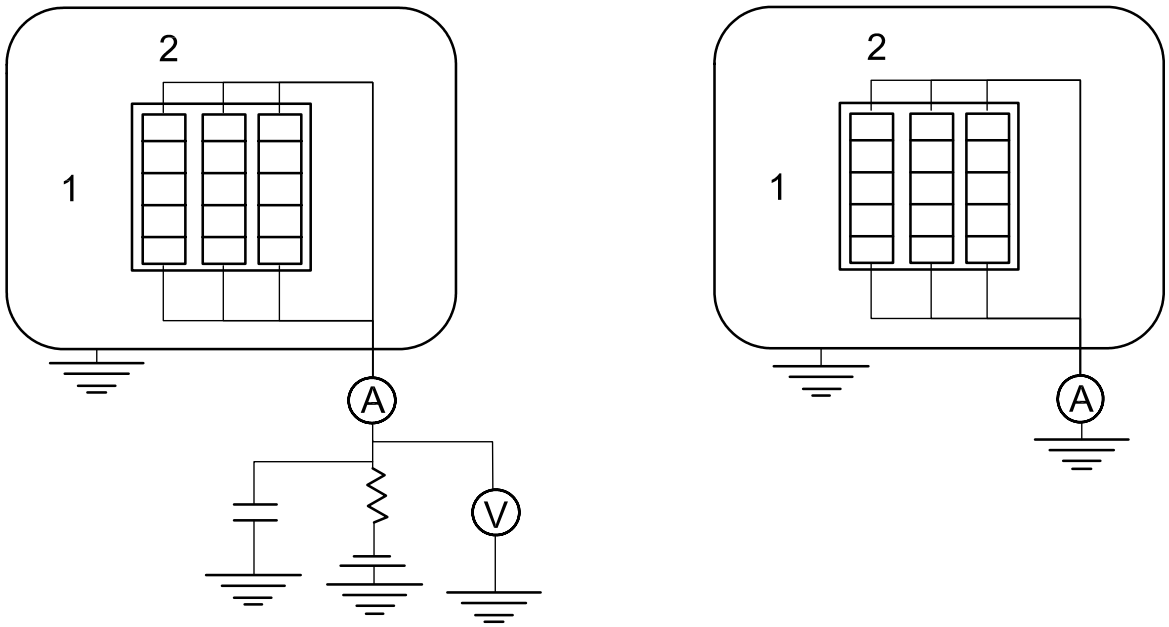

a) Inverted potential gradient **b) Normal potential gradient**

Key

1 coupon

2 vacuum chamber

Figure 4 — Test set-up for the ESD inception test

6.5 Test procedures

If an electron beam gun or a UV source is used for charging the test coupon, the test shall be carried out until a statistically significant number of ESD events, no less than 10, occur on the test coupon. The test coupon surface potential shall be measured repeatedly during the test by a non-contacting surface potential probe. The coupon surface potential closest to each ESD location shall be identified and recorded. The minimum differential voltage is the minimum value among all the ESD events recorded. Be aware of the uncertainties associated with the spatial resolution of the probe and the temporal variation of the potential depending on the time of measurement from the ESD inception.

If a low-energy plasma source is used, the differential charging voltage can be approximated by the chamber plasma potential, which is usually positive by several times the electron temperature, minus the negative coupon potential. The uncertainty is in the order of the electron temperature. The coupon bias voltage shall be varied to cover all the possible charging potentials in orbit. In the case of PEO spacecraft, the waiting time at each bias voltage should be no less than 20 min. In the case of LEO spacecraft, the waiting time at each bias voltage should be no less than 90 min. At low bias voltages where the probability of ESD is very low, a longer waiting time is recommended to improve the statistics. See Reference [1] for an example of characterizing the arc rate per unit time under a low-energy plasma environment. If the threshold is unknown, plot the arc rates at different bias voltages on a logarithmic scale and find the voltage where the probability of an arc over a given time becomes negligible, assuming that ESD inception is modelled as a Poisson process (see Reference [2] for an example).

6.6 Estimation of number of ESD events in orbit

It can be useful to analyse the number of ESD events expected in orbit as a basis for discussion to determine the number of primary discharges in the subsequent tests. See Annex D for details. Other methods of analysis may also be used to compute the number of ESD events.

7 Qualification test for secondary arc

7.1 Purpose

The purpose of this test is to qualify a given design of solar panel for flight. The purpose of the coverglass interconnect cell (CIC) gap test (7.4) is to demonstrate that no damaging secondary arc occurs even when primary discharges are forced to occur directly on the active CIC gap, which is a possible worst case scenario. The purpose of the panel test (7.5) is to show that no damaging secondary arc occurs, even after a significant number of primary discharges occur all over the flight-representative test coupon. See Annex B for a more detailed rationale of both tests.

It may not always be possible to replicate the orbital worst case scenario in the laboratory experiment (e.g. low temperature at the end of eclipse, the effects of thermal cycling on gap distance, failure or aging of grouting, and the outgassing time period in orbit). However, every effort shall be made to simulate the worst case scenario or to extrapolate the test results to represent the worst case scenario parametrization.

7.2 Triggering method and test facility

If it can be confirmed that the probability of a transition from a primary discharge to a secondary arc does not depend upon the method of primary discharge inception, any method may be used to cause primary discharges, irrespective of the anticipated charging situation in orbit. If the transition probability depends upon the testing plasma environment, the same test facility as used for the primary discharge inception threshold test shall be used. In either case, the shape and amplitude of the primary discharge current in the test shall be plausibly representative of the current expected in orbit.

There is a risk of primary discharge and subsequent secondary arcs in LEO even for a GEO spacecraft as it passes through LEO during the orbit transfer. Also, if a plasma emission device is used, such as a plasma contactor, LEO-type arcing may occur when the device is first turned on or off. Therefore, for a GEO spacecraft, the test should be performed under the conditions in a LEO-type plasma in addition to the GEO-type test. See Annex C for the minimum chamber size for a low-energy plasma test.

The test shall take place under vacuum in a test chamber with a pressure that guarantees the physical state of a collisionless plasma if a low-energy plasma is used, or lower than 3×10^{-3} Pa if other triggering methods, such as an energetic electron beam, UV ray, laser pulse, etc., are used. Care should be taken to choose a power supply capable of reproducing the dynamic response of the array to transient short circuits (such as limited overshoot current and fast recovery to the steady state). Simultaneous ESD current transient monitoring and recording devices and a video imaging device are also required for the test.

7.3 External circuit

The cells need not be illuminated, but the available current and capacitance shall be simulated by power sources and external capacitors, C_{sat} and C_{CG}, representing the satellite capacitance and solar array coverglass capacitance respectively. The capacitance of the missing coverglasses shall also be factored into the test. The current waveform supplied by the external circuit shall be representative of the surface flashover current in orbit. Under the present state of knowledge, the propagation distance is taken to be 2 m, confirmed by a laboratory test using a 4 m × 1 m coupon panel (see Reference [3]). The present best estimate of the propagation speed of surface flashover is 10 km/s for a GEO solar array under inverted potential gradient. See Annex F for an example of the current waveform derivation. The electric architecture of a solar paddle shall be taken into account to determine the waveform. If a mitigation method for flashover current is included in the design, the effect shall be taken into account in sizing energy in the capacitance C_{CG}.

The inductance of the wire harness should be representative of a flight solar panel. Excessive inductance shall be avoided as it affects the transient current waveform. Short cable lengths or coaxial cables reduce the unwanted inductance. Annex G specifies the external circuit for use in the case of inverted potential gradient. If testing under normal potential gradient is imperative, a representative flashover current to the primary discharge shall be provided.

7.4 CIC gap test — Test coupon and procedures

The test coupon(s) shall consist of at least two strings of two cells to represent a point surrounded by solar cell corner edges. The total number of test coupon(s) shall reflect the production variation, including reworked cells. The solar cells shall be laid down on the substrate in the same manner as for the flight model. The substrate shall also be made of the same material as the flight model. If the solar panel design includes ESD inception mitigation, whether the mitigation design is included in the test coupon or not depends on definition of the worst case scenario in orbit. If failure of the mitigation method is regarded as the worst case scenario, the mitigation method may be removed from the coupon. Before and after the test, the tasks specified in Table 1 shall be carried out.

The primary discharges may be concentrated on the cell gap. The test shall ascertain that a significant number of primary discharges (at least three, or more than three if agreed with the customer on the basis of statistical discussion; see Reference [4] for an example) per given test condition occur in the active gap or in the vicinity of the active gap if a grouted gap is tested.

Table 1 — Required tasks before and after the ESD test

Item	Before test	After test	Comment
Visual inspection of the coupon	x	x	With optical microscope
Output power measurement	x	x	Same light source
Insulation check across the cell gap	x	x	By measurement
Insulation check between the cells and the substrate	x	x	

7.5 Panel test — Test coupon and procedures

The test coupon shall consist of at least three strings of three cells to represent means of cell surrounded by other cells. The coupon shall be a flight-representative qualification coupon covering the production variation of the string gap distance and CIC cell configuration (coverglass overhang, adhesive thickness, etc.), including reworked cells. The solar cells shall be laid down on the substrate in the same manner as for the flight model. The substrate shall also be made of the same material as the flight model. If the solar panel design includes ESD inception mitigation, the mitigation design should be included in the test coupon so as to be as flight-representative as possible. Before and after the test, the tasks specified in Table 1 shall be carried out.

The total number of primary discharges on the coupon shall be determined by means of statistical analysis. The total number of ESD events, as derived in accordance with Annex D, is useful in determining the number of primary discharges. No control shall be carried out at the primary discharge locations.

7.6 Success criteria

The test shall demonstrate that no damaging secondary arc occurs due to ESD.

8 Characterization tests for robustness to ESD and plasma interaction

8.1 Power degradation

8.1.1 Purpose

The purpose of this test is to characterize power degradation due to repeated ESD events after the desired orbital lifetime. As the present knowledge about the power degradation is not mature enough to list power degradation as a qualification item, the power degradation is measured for characterization purposes only.

This test may be performed simultaneously with the coupon panel test (7.5) provided the test requirements listed in 7.2, 7.3 and 8.1 are satisfied.

8.1.2 Test facility

The test facility shall be the same as the one used for the ESD inception threshold test (6.2).

8.1.3 Test coupon

The CIC solar cells on the test coupon(s) shall be of flight quality. The definition of flight quality shall be agreed upon with the customer prior to the test. The solar cell, coverglass, adhesive (both for coverglass and substrate) and interconnector shall be of the same type and material as for the flight models. The illuminated current-voltage (I-V) characteristics before the test shall be in accordance with the customer's specification of flight quality. The substrate need not be of the same material as the flight model. The total number of test coupon(s) shall reflect the production variation, including reworked cells.

8.1.4 External circuit

An external circuit shall provide additional electrostatic energy that would have been provided by the insulator capacitance not accommodated inside the vacuum chamber. The current waveform supplied by the external circuit shall be representative of the surface flashover current in orbit. Under the present state of knowledge, the propagation distance is taken to be 2 m, confirmed by a laboratory test using a 4 m $\times$ 1 m coupon panel (see Reference [3]). The present best estimate of the propagation speed of surface flashover is 10 km/s for a GEO solar array under inverted potential gradient. See Annex F for an example of the current waveform derivation. The electric architecture of a solar paddle shall be taken into account in determining the waveform.

8.1.5 Test procedures

Illuminated current-voltage (I-V) characteristics shall be measured pre- and post-test with an appropriate light source. The intensity of the light source shall be calibrated using a reference cell so that the relative change of the power output can be measured precisely. The exact conditions of the illuminated I-V measurement shall be based on an appropriate solar cell calibration standard, selected in agreement with the customer prior to testing. A visual inspection shall be performed pre- and post-test using an optical microscope. The test can be terminated once it satisfies one of the following:

a) the estimated number of ESD events during the mission in orbit (see 6.6) occurs;

b) ten discharges for any one cell do not create cell degradation;

c) a predetermined number of ESD events, as agreed with the programme customer, occurs.

It is advisable to measure dark current with a DC power supply in order to perform in situ monitoring of the progress of degradation during the test by comparing the dark current with the pre-test value. See Annex H for more information on the measurement of the dark current. The total drop of spacecraft power at the end of its mission lifetime shall be derived and recorded.

8.2 Secondary arc

8.2.1 Purpose

The purpose of this test is to characterize the secondary arc for a given design of solar panel. The characteristics include the probability of transition from a primary discharge to a secondary arc and the duration of the secondary arcs if the transition probability is not zero. If the characteristics are already known from past experience, this test is not necessary to qualify the solar panel for secondary arcs.

8.2.2 Triggering method and test facility

The triggering method and test facility shall be as specified in 7.2.

8.2.3 Test coupon

The test coupon(s) shall consist of at least two strings of two cells to represent a point surrounded by solar cell corner edges. The total number of test coupon(s) shall reflect the production variation, including reworked cells. The cell gap spacing should be kept within an allowable design tolerance from the specification. The solar cells shall be laid down on the substrate in the same manner as for the flight model. The substrate shall also be made of the same material as in the flight model.

If the solar panel design includes ESD inception mitigation, whether the mitigation design is included in the test coupon or not depends on the definition of the worst case scenario in orbit. If failure of the mitigation method is regarded as the worst case scenario, the mitigation method may be removed from the coupon.

8.2.4 External circuit

The external circuit shall be as specified in 7.3.

8.2.5 Test procedures

Before and after the test, the tasks specified in Table 1 shall be carried out. Primary discharges may be concentrated on the cell gap. For each pair of gap voltage and string current agreed upon with the customer, the probability of transition from primary discharge to secondary arc shall be derived. The test shall ascertain that at least ten primary discharges per given test condition occur in the active gap (or in the vicinity of the active gap in the case of a grouted gap). If it is necessary to identify the confidence level of the transition probability, a significant number of primary discharges (as agreed with the customer on the basis of statistical discussion) per the given test condition shall occur in the active gap. If the transition probability is not zero, statistics of secondary arc duration, such as the mean and the standard deviation, are useful to extrapolate the probability of a damaging secondary arc with a very long duration. If any statistical distribution function is proposed to describe the secondary arc duration, its goodness-of-fit shall be determined by an appropriate method, such as the χ^2 statistic. See Annex I for an example of deriving the statistics.

8.3 Power leakage to plasma

8.3.1 Purpose

The purpose of this test is to characterize the power leakage from a solar array to the surrounding plasma. The plasma density and neutral gas density near the spacecraft shall be analysed first. Charging analysis tools employing a particle simulation method (see Annex E) can estimate the amount of current for a given plasma density. A rough estimate of the critical neutral gas density for transition of snapover to neutral gas ionization can be obtained using formulas in References [5] and [6]. If the power leakage due to snapover is low and neutral densities are too low for snapover to lead to neutral gas ionization, this test is not necessary.

8.3.2 Test facility

The test shall take place under vacuum in a test chamber equipped with a low-energy plasma source capable of generating the plasma density expected around the solar array in orbit. The plasma species do not have to be the same as those in orbit (see Reference [2]) A best effort shall be made to realize a plasma temperature similar to the value in orbit. If the plasma temperature is higher than that in orbit, the test result on the collected current shall be corrected based on either computer simulation or theory. The neutral background pressure shall be kept below 0,01 Pa so that unrealistic electron-neutral collisions do not affect the test results. The test facility shall be equipped with a DC power supply capable of supplying several amperes of current at several hundred volts, a recording device to monitor the collection current and the coupon potential simultaneously, a video imaging device and a plasma diagnostic device to determine the chamber plasma properties including the plasma potential with respect to the chamber wall. See Annex C for the minimum chamber size for a low-energy plasma test.

8.3.3 Test coupon

The number of CIC solar cells per coupon shall be as many as is practical. The minimum number shall be at least three strings of three cells. The use of mechanical CIC cells (not electrically flight-like) is acceptable as long as all the conductive parts, including the cell edge and interconnector, are exposed in the same manner as the flight model. The substrate material shall be flight-representative. The total number of test coupon(s) shall reflect the production variation including reworked cells.

8.3.4 External circuit

Both ends of the positive and negative electrodes of an array may be combined and connected to a DC power supply as illustrated in Figure 5. The cells need not be illuminated during the test.

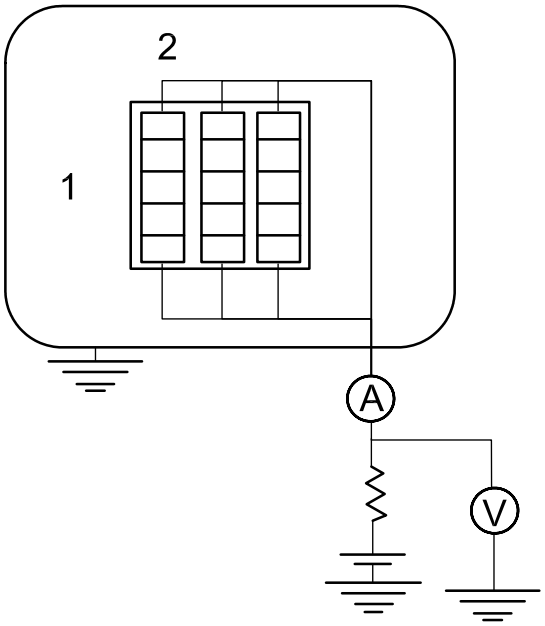

Key

1 coupon

2 plasma chamber

Figure 5 — Schematic of circuit diagram for the characterization test of plasma power leakage

8.3.5 Test procedures

Before the test, the solar array coupon shall be visually inspected with an optical microscope. The test coupon bias voltage shall be changed step-wise while monitoring the potential of the coupon with respect to the plasma potential until the potential reaches the maximum solar array output voltage in orbit. The current collected at each potential shall be recorded after the current has become steady. After the test, the visual inspection shall be repeated. The overall power leakage from the spacecraft to the plasma shall be derived and reported.

8.4 Solar array back surface test

Although the scope of this International Standard is surface discharge and plasma interaction on the solar array front surface, the possibility of ESD and plasma interaction on the solar array back surface cannot be excluded (see Annex J).

9 Test report

The ESD test report shall include the following elements:

a) a title;

b) a description of the test facility (i.e. chamber size, chamber pressure, power supply, recording device, etc.) with photographs of the test set-up; verify that all necessary facility criteria are met;

c) a description of the test coupon (i.e. solar cell type, solar cell output power, number of coupons tested, etc.);

d) a description of the test conditions as follows:

   1) when a low-temperature plasma is used, the plasma conditions, such as plasma density, temperature and potential, shall be listed;

   2) when an electron beam is used, the beam energy and current density shall be listed;

   3) if the coupon is placed in a vacuum chamber for outgassing purposes prior to the test, the duration, pressure and temperature shall be listed;

   4) the coupon temperature during the test shall be reported;

e) external circuit diagrams for each test case, identifying the value of each circuit element (any floating capacitance and inductance involved in the circuits should be identified);

f) the test results as follows:

   1) summarize all visual inspections and include photographs of the test coupons before and after the tests;

   2) ensure that plots of test results have error bars in order to ascertain uncertainties in the test(s) where applicable;

   3) include appropriate analyses and discussion of observations and results;

g) a summary of qualification tests, with an indication whether the solar panel has passed or failed qualification;

h) a summary of characterization tests where applicable, including the derived total drop of spacecraft power at the end of mission lifetime, the transition probability to a secondary arc, the duration of secondary arc and the derived overall power leakage from the spacecraft to the plasma.

Annex A
(informative)

Plasma interaction and electrostatic discharge effects on solar array

A.1 Plasma environment in orbit

For details of the orbital plasma environment, see References [7], [8], [9], [10], [11] and [12]. Generally speaking, GEO is characterized by the presence of electrons with energies greater than 1 keV. Under quiet conditions, the electron current is less than the photoelectron current, which is of the order of 1 $\mu A/m^2$ to 10 $\mu A/m^2$, and there is no serious surface charging issue. Under stormy conditions, the electron current exceeds the photoelectron current, and the risk of electrostatic discharge on the solar array surface increases. Several examples of the worst case GEO plasma environment can be found in Reference [13]. LEO is characterized by the presence of low-energy but dense ionospheric plasma where the particle density is of the order of 10^8 m^{-3} to 10^{12} m^{-3}. For an object at the plasma potential in LEO, current from electrons of energies 0,1 eV to 0,2 eV dominates over any other current source to the spacecraft. The spacecraft body's potential floats with respect to the ionospheric plasma potential, at an absolute value smaller than the solar array power generation voltage. PEO is characterized by auroral electrons with energies greater than 1 keV that coexist with the low-energy ionospheric plasma. In some cases, the auroral electron current, which can be as large as 1 mA/m^2, may dominate over the other current sources and drive the spacecraft body to a potential more negative than the power generation voltage. When a spacecraft is equipped with an electric propulsion system, the artificial plasma can dominate the plasma environment around the spacecraft, especially in GEO.

A.2 Spacecraft surface charging

The spacecraft body that is made of conducting material serves as a grounding point in the spacecraft circuit. Currents to/from conductive parts exposed to space, and the capacitance between the spacecraft body and ambient space, determine the body potential with respect to the ambient space plasma. As the solar array circuit is also grounded to the spacecraft body, any point on the solar array circuit has a potential close to the spacecraft body's potential within the power generation voltage. When the negative end of a solar array circuit is grounded, the potentials on the solar array conductive parts have a distribution from the body potential to the body potential plus the power generation voltage.

In GEO, differential charging on the solar array surface can develop when the spacecraft encounters a high flux of energetic electrons. Conductive parts of the solar array, such as the solar cell electrode, interconnector or bus-bar, have a negative potential bounded by the spacecraft body potential. Insulator parts, such as the coverglass, adhesive or facesheet, also have negative potentials, but the values can be different from the body potential by 1 kV or greater. In PEO, a situation similar to GEO may arise when the spacecraft encounters the aurora and the solar array front surface is facing the wake side. When the solar array front surface is facing the ram side in PEO, the aurora can drive the spacecraft body potential negative and the insulator surface can be charged by ionospheric ions to a potential close to the ambient plasma potential. In LEO, differential charging on the solar array surface appears as the insulator parts have potentials close to the ambient plasma potential and the conductive parts have potentials ranging from the negative of the power generation voltage to the positive of the power generation voltage. Therefore, for LEO spacecraft, ESD and PI issues arise only when the power generation voltage exceeds the primary arc or snapover threshold voltage.

Spacecraft surface charging can be assessed with the aid of computer simulations. There are several computer programs that can calculate the differential voltage for a given set of spacecraft geometry, environmental parameters and surface material properties. As ESD occurs during a transient phase of differential charging in GEO and PEO when a differential voltage develops due to an encounter with a substorm or aurora, it is important for the programs to be able to calculate the transient behavior in addition to the steady state behavior. See Annex E for examples of such software. Although the computer simulation tools can give the differential voltage, they cannot predict the discharge inception voltage.

A.3 Electrostatic discharge on solar array

ESD on a solar array is a single, fast, high-current transfer of electrostatic charge that results from a strong electrostatic field between two objects in close proximity. Differential charging on solar array exterior surfaces builds up an electric charge on the insulator surface. The electrostatic energy stored on the insulator is partially or fully released once the electric field on any part of the surface exceeds the discharge inception threshold. ESD has three forms of current path. The first is blow-off, which is the emission of negative charges (electrons) into space. The blow-off current discharges electric charge stored in the capacitance between the spacecraft and the ambient plasma. The second is flashover, which is a surface discharge propagating from a starting point as the surface of the dielectric becomes conductive (by the creation of a plasma). The flashover current discharges electric charge stored in the capacitance between the surface of an insulator and the spacecraft ground. The third is punch-through, which is the classic breakdown of a dielectric material, such as the breakdown of a capacitance, for example. The punch-through discharge neutralizes not only electric charge stored in the capacitance between the insulator and spacecraft ground, but also some of the electric charge stored inside the insulator material due to penetrating charged particles. Considering the thickness and dielectric strength of typical insulator materials used on solar arrays, blow-off or flashover-type discharge is more likely to occur than the punch-through discharge.

The inception threshold for ESD on a solar array is often measured by the potential difference between the coverglass surface and the spacecraft ground. Although the threshold depends upon numerous parameters such as polarity, geometry, material, ambient atmosphere, etc., the inverted potential gradient (IPG) situation has a smaller threshold (hundreds of volts) than the normal potential gradient (NPG) situation (thousands of volts). IPG ESD has been more thoroughly investigated than NPG ESD. For high-voltage LEO spacecraft, IPG is the nominal condition. In PEO and GEO, the secondary electron and photoelectron coefficients of insulator material determine the polarity. As the solar array is illuminated by sunlight during power generation, and the coverglass coating, such as MgF_2, has a very high secondary electron coefficient, IPG is expected to occur more frequently than NPG. As the situation can differ for each spacecraft, however, a charging analysis should be carried out to determine the polarity on the solar array for each spacecraft unless an identical spacecraft design is employed.

Normal or inverted, ESD originates from a micro-discharge at its inception point. For IPG, it is believed to be due to the field emission and desorption of gas near the so-called triple junction, where the insulator material, conductor and vacuum (plasma) meet together (see References [14], [15] and [16] for more details). For NPG, it may be due to punch-through of a thin dielectric or an electron avalanche triggered by seed electrons produced by various reasons. Due to the negative potential of the spacecraft body and the high mobility of electrons, the blow-off current quickly discharges the satellite capacitance (absolute capacitance), with typical values from 100 pF to 1 000 pF. The flashover current follows the blow-off by neutralizing electric charge on the insulator near the ESD inception point. In the case of IPG, the flashover current flows to the inception point and forms cathode spots, transforming the ESD into a form of vacuum arc. Therefore, IPG ESD is called a primary arc. The primary arc receives its energy from the electrostatic energy stored in the capacitance between the insulator surface and the spacecraft body (differential capacitance), which is typically much greater than the absolute spacecraft capacitance.

A.4 Detrimental effects of ESD

ESD on a solar array can cause various detrimental effects to the solar array operation. The large transient current can cause electromagnetic interference with spacecraft circuits. As ESD can occur repeatedly during the lifetime of a spacecraft, there can be cumulative effects such as surface degradation, surface contamination via vaporized material or internal damage to solar cells due to surge voltages. When ESD occurs at the edge of a solar cell or bypass diode, it may degrade their electrical performance.

“Primary discharge” includes both IPG ESD (primary arc) and NPG ESD that can trigger a secondary arc. The primary discharge is fed by the absolute and differential capacitances. The primary discharge can create a temporary conductive path between any two cells with different voltages generated by the solar array. The current between the two cells can become sustained when fed from the solar array output power. This resulting phenomenon is called a “secondary arc”. The secondary arc is powered by an illuminated solar array and leads to an important additional damage mechanism since the solar array circuit can become permanently short-circuited.

The secondary arc can be self-sustained or not. There are several stages of a secondary arc, as illustrated in Figure 1. Figure 1 illustrates examples of the current waveform seen in secondary arc tests. The primary discharge current is seen as the blow-off current flowing from the external capacitance to the chamber wall through the solar cells. The secondary arc current is seen as the arc current flowing between the two cells through the external power supply that simulates the illuminated solar array. In the Figure 1, I_{SC} represents the short-circuit current of one or more of the solar array circuits. A non-sustained arc (NSA) is a secondary arc that lasts only during the primary discharge. It ends when the primary discharge stops. A self-sustained arc is a secondary arc that lasts longer than the primary discharge. A temporary sustained arc (TSA) is self-sustained but it stops by itself even though the solar array power is still available. A permanent sustained arc (PSA) is an arc that does not stop while the solar array power is available. PSA can last for seconds or longer. The very intense heat in the vicinity of the secondary arc creates a highly conductive path by pyrolizing materials around the discharge site. When a solar array is laid down on an insulator face-sheet over a conductive substrate, a pyrolized insulator leaves a permanent conductive path even after the external power is shut off. The solar array circuit then remains short-circuited to the solar panel ground, diverting the solar array power to the panel ground.

A.5 Power leakage from solar array to plasma

The use of a potential control device, such as a plasma contactor, can mitigate ESD-related charging problems on a solar array by raising the satellite body potential to a level close to the ambient plasma potential. At the same time, however, it can lead to the problem of excess power leakage, especially in LEO. The power leakage may also be a problem for a spacecraft with a plasma thruster system that is tied to the spacecraft chassis, regardless of its orbit. Exposed conductive parts of a solar array collect electrons if their potential is positive with respect to the ambient plasma potential. Part of the solar array power drains into the plasma circuit. The part of the solar array current that is diverted into the plasma is sometimes called the parasitic current.

As most of a solar array's surface is covered with a dielectric coverglass, the exposed conductor usually makes up a tiny portion of the array area. As long as the voltage between the positive conductive parts and the plasma is low, electron collection current is limited by the geometry and scales only linearly with the voltage. As the voltage becomes higher, however, current collection increases exponentially and finally saturates at a current level that is approximately the same as if the entire plate were conducting. The transition is quite striking with conventional solar array designs and has been called “snapover”. When the ambient neutral pressure is high, snapover may be combined with a glow discharge that further increases the electron current. Once the snapover or the glow discharge occurs, power leakage to the plasma is no longer negligible.

Annex B
(informative)

Secondary arc qualification processes

Before drafting of this International Standard on solar panel ESD test procedures began, various styles of ESD tests had already been carried out in various countries (see References [17], [18], [19], [20], [21], [22] and [23] for examples). In some countries, the emphasis was on making sure that the devastating secondary arc would not occur even under the worst possible conditions. In those countries, the worst case scenario was often assumed to be a primary discharge at the active gap and, if the gap was grouted, the worst case scenario was assumed to be failure of grouting, i.e. no grouting. The CIC gap test described in 7.4 is based on the test procedure adopted in those countries. In other countries, the qualification tests had been performed under the philosophy of “test as you fly”. Therefore, the coupon panel test that employs a test coupon which is as flight-representative as possible, without any modification to increase the probability of primary ESD occurrence at the active gaps, has been regarded as mandatory in addition to the CIC gap test. The coupon panel test described in 7.5 is based on the test procedure adopted in those latter countries working on the “test as you fly” principle. Although intensive efforts have been made to absorb the difference between the test methods carried out in different parts of the world, in order to be able to produce this International Standard within a limited time frame, it was necessary to adopt the test flow structure shown in Figure 2.

Annex C
(normative)

Chamber size for a test using LEO-like plasma

The minimum acceptable plasma chamber dimension in a given direction for a centrally located sample is the sample dimension in that direction plus two plasma Debye lengths, plus the plasma sheath widths at the sample bias. No exposed grounded conductor should be located within one plasma sheath width plus one Debye length from the active surface of the sample. Figure C.1 illustrates the requirement schematically. Having a sample surrounded by the plasma is critical for the power leakage test.

For ESD, the plasma sheath acts as a virtual anode. The majority of the ESD current is carried by the flashover. The flashover current in orbit flows between the ESD inception point and the coverglass surface. Therefore, making the plasma sheath size the same as in orbit is not critical in the ESD test.

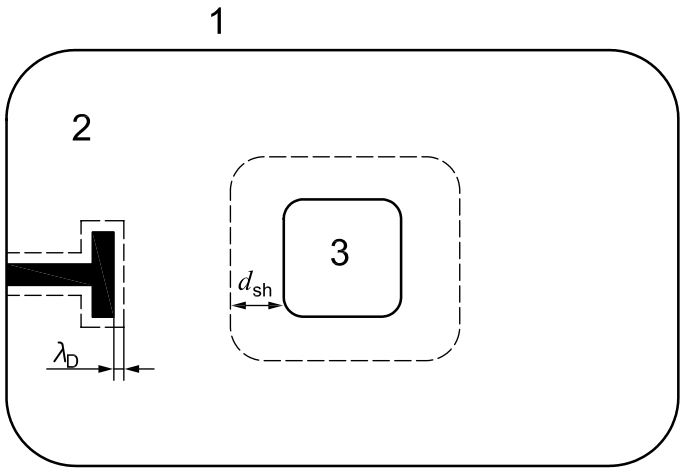

Key

1 chamber wall
2 plasma
3 sample

d_{sh} sheath thickness
λ_D Debye length

Figure C.1 — Minimum acceptable chamber size for a test using LEO-like plasma

Annex D
(informative)

ESD events analysis

In order to have a statistical discussion about the test conditions or the test results, it is useful to know the likelihood of ESD events in orbit. Spacecraft charging in orbit can be analysed to determine whether the predicted voltage differentials will exceed the ESD inception threshold. This can be done by consulting a database to compute the probability of the charging environments the spacecraft may encounter. The charge differential is then computed for these cases together with the time it takes to achieve the differential. There are several computer programs, examples of which are listed in Annex E, that can perform these calculations. At the very least, the charging simulation for the worst charging environment should be run (see References [9] and [24]).

The number of ESD events in orbit can be estimated as follows[25]:

a) list the space plasma environments that a given spacecraft will encounter in orbit;

b) carry out spacecraft charging analysis for each type of space plasma environment;

c) identify plasma environment cases that give a differential voltage exceeding the ESD inception threshold;

d) for each case identified in c) above, calculate the charging time necessary to reach the threshold value;

e) derive the probability of occurrence of each case identified in c) and the expected total duration in orbit;

f) divide the expected total duration obtained in the e) by the charging time obtained in d) to obtain the expected number of ESD events for each case exceeding the ESD inception threshold;

g) sum the number of ESD events to derive the total number.

More details can be found in Reference [25].

For the steps given in a) and e) above, a proper database relating to the space plasma environment should be consulted. An example of a GEO database is the Los Alamos National Laboratory (LANL) satellite data, which is available on the internet (see Reference [26]), where the magnetospheric plasma analyser (MPA) data are listed for electron density, electron temperature, ion density and ion temperature between 1 eV and 45 keV. These have been measured by multiple LANL satellites every 90 s since 1993. An example of a PEO database is the Defense Meteorological Satellite Program (DMSP) satellite data. These auroral electron data are available on the internet (see Reference [27]), and include the SSJ/4 (Precipitation Electron/Proton Spectrometer) data for the precipitating electron flux between 30 eV and 30 keV, measured by multiple DMSP satellites at an altitude of approximately 840 km every 1 s since 1983. LEO ionospheric data are available on the internet from Reference [28], where the Special Sensor-Ions, Electrons, and Scintillation (SSIES) data are listed for electron density, electron temperature, ion density and ion temperature, measured by multiple DMSP satellites every 4 s since 1987.

In the step given in b) above, a proper spacecraft charging analysis tool should be used. Annex E provides a list of the computer programs currently available. The differential voltage between the coverglass and the spacecraft body should be calculated for a given set of the environmental parameters. The worst case scenario should be calculated first, as there will be no need for further analysis and an ESD test if the worst case simulation shows no possibility of the differential voltage exceeding the ESD inception threshold. (If the ESD threshold is not known, it should be determined by testing.) It should be noted that the result of a charging analysis often depends strongly on spacecraft material properties. Even if the worst case simulation shows no serious charging, the result should be confirmed by varying the material data over the entire possible range of the parameters.

Figure D.1 illustrates how the charging time can be calculated in step d) above. In this example, the NASA Charging Analyzer Program NASCAP/GEO was used to calculate charging for a GEO satellite. Figure D.1 also lists the plasma parameters. The simulation starts from the condition where both the satellite and coverglass potentials are zero. As the charging starts, the differential voltage gradually builds up. If the ESD inception threshold is 400 V, the threshold is reached in 20 s (in this example). Once the threshold is attained, an ESD occurs somewhere on the solar paddle and the satellite body potential goes back to zero. By assuming that the differential charging is initialized by one ESD, the process of charging and ESD is repeated as long as the harmful plasma environment continues.

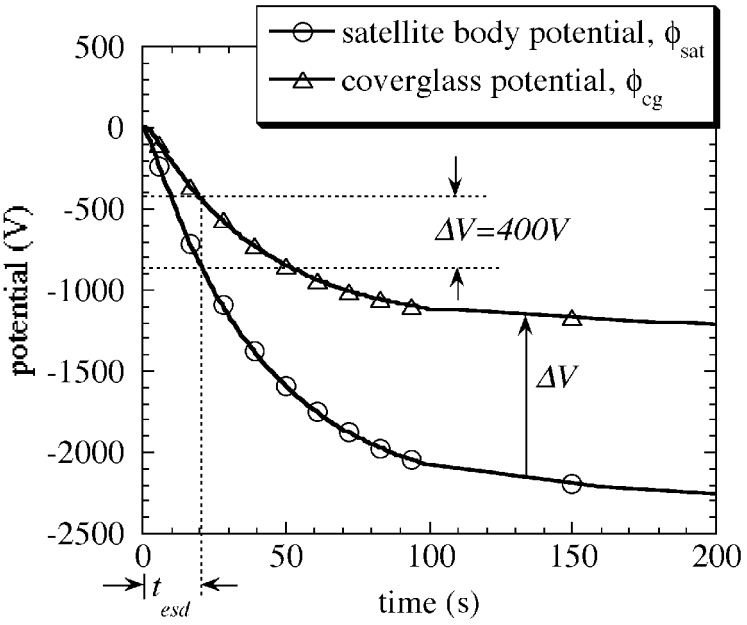

Key

t_{ESD} time to threshold differential voltage

ΔV potential difference

NOTE Plasma parameters: T_e = 7,5 keV; ρ_e = 10 cm^{-3}; T_i = 10 keV; ρ_i = 0,25 cm^{-3}.

If the ESD inception threshold is 400 V, the time to reach the threshold differential voltage (t_{ESD}) is 20 s for this case (see Reference [25]).

Figure D.1 — Example of charging profile calculated for a GEO satellite[25] 1)

Table D.1 illustrates how the number of ESD events in one year is derived. Using the result of the statistical analysis in step e) above, the expected duration of each plasma environment can be calculated for each local time zone in GEO. For each case, the charging analysis calculated in step d) provides the time to reach the threshold. In Table D.1, N/A indicates that the differential charging does not reach the threshold value even at the steady state. The number of ESD events for each case is calculated by dividing the duration by the time needed to reach the threshold.

1) Reprinted with permission from AIAA.

Table D.1 — Example of derivation of the number of ESD events for a GEO satellite[25] 2)

Plasma parameters				Duration in one year, s					Time to reach ΔV = 400 V, s					Number of arcs in one year				
T_e, keV	ρ_e, cm^{-3}	T_i, keV	ρ_i, cm^{-3}	LT0e	LT0n	LT6	LT12	LT18	LT0e	LT0n	LT6	LT12	LT18	LT0e	LT0n	LT6	LT12	LT18
13,5	5	5	0,25	0	290	106	439	33	8	9	10	9	9	0	32	11	49	4
10,5	10	10	0,25	0	0	448	156	29	5	6	6	6	6	0	0	75	26	5
10,5	5	10	0,25	4	55	558	507	194	9	12	12	12	12	0	5	47	42	16
10,5	5	5	0,25	0	154	321	405	70	9	12	12	12	12	0	13	27	34	6
7,5	10	10	0,25	4	13	220	329	70	7	8	8	8	8	1	2	28	41	9
7,5	10	5	0,25	0	34	313	173	83	7	8	8	8	8	0	4	39	22	10
7,5	5	10	0,25	8	111	1 848	925	112	13	18	20	19	18	1	6	92	49	6
7,5	5	5	0,25	4	145	773	650	157	13	18	20	19	18	0	8	39	34	9
4,5	10	10	0,25	0	38	525	215	21	13	20	22	21	20	0	2	24	10	1
4,5	10	5	0,25	0	90	399	177	103	13	20	22	21	20	0	5	18	8	5
4,5	5	10	0,25	0	175	0	3 184	673	26	140	N/A	170	140	0	1	0	19	5
4,5	5	5	0,25	4	249	0	887	549	26	120	N/A	140	120	0	2	0	6	5
4,5	5	1,25	0,25	0	148	0	0	0	26	110	N/A	130	110	0	1	0	0	0

T_e Electron temperature.

ρ_e Electron density.

T_i Ion temperature.

ρ_i Ion density.

LT Local time.

N/A Not applicable. The simulation did not reach ΔV = 400 V.

2) Reprinted with permission from AIAA.

Annex E
(informative)

Spacecraft charging analysis

E.1 General

There are a number of simulation codes available for performing surface charging assessments taking into account surface material processes or 3D effects. Historically, the most common spacecraft charging analysis code in use by the space industry was NASCAP/GEO, developed by NASA and the US Air Force. It has been made available to various users via collaboration agreements with NASA or via commercial arrangement. Although NASCAP/GEO has been replaced by NASCAP-2K in the United States, NASCAP-2K is subject to export restrictions. Recently Japan Aerospace Exploration Agency (JAXA) has sponsored the development of the Multi-Utility Spacecraft Charging Analysis Tool (MUSCAT) and the European Space Agency (ESA) has sponsored the development of the Spacecraft Plasma Interaction System (SPIS).

The basic objective of spacecraft surface charging analysis is to calculate the contribution of each current component by following the trajectories of the ambient plasma particles, calculating the interaction between the incident particles and the surface material and considering the emission of charged particles from the surface, such as secondary electron, photoelectron and artificial plasmas. Then, the surface charge distribution is updated based on the current density and conductivity of each surface element relative to the spacecraft body ground. The surface potentials are calculated by solving the Poisson equation or the Laplace equation. Particle trajectories are recalculated for the renewed surface potential and the processes are repeated until the elapsed time reaches the predetermined time or the steady state is obtained. The important features of the charging analysis code are the capability to model the three-dimensional geometry of the spacecraft and significant surface interactions such as secondary electron and photoelectron emission, and a database relating to spacecraft surface material properties such as conductivity, secondary electron emission yield and photoelectron emission coefficient.

E.2 Examples of spacecraft charging analysis codes

E.2.1 NASCAP/GEO

NASCAP (also called NASCAP/GEO; see Reference [29]) is commonly used for simulating surface charging in the outer magnetosphere. This code calculates the total current, due to all the current contributions, for each surface on a numerically modelled 3D spacecraft, using a double Maxwellian environment for both ions and electrons. From these currents, the change in potential at each surface is calculated. The current and potential calculations can be performed iteratively until an equilibrium charging state is achieved. The code is available commercially upon request from Science Applications International Corporation, USA.

E.2.2 NASCAP/LEO

NASCAP/LEO is aimed at the simulation of high-potential objects with a cold, dense plasma typical of the LEO environment. Like NASCAP/GEO, it employs analytical current collection equations, although these are aimed at sheath-limited current collection and are appropriate for the short Debye-length LEO plasmas. Typical uses are the simulation of parasitic currents from high-potential surfaces, such as solar array interconnects. The geometrical model of the spacecraft is more sophisticated than for NASCAP/GEO, consisting of a finite-element representation. The code is available commercially upon request from Science Applications International Corporation, USA.

E.2.3 POLAR charging code

The main problem with computing charging in LEO is due to effects associated with the spacecraft sheath. The 3D POLAR code (see Reference [30]) has been designed for the assessment of sheath and wake effects on PEO spacecraft. It uses numerical techniques to track ambient ions inwards from the electrostatic sheath surrounding a negatively charged spacecraft onto the spacecraft surface. The spacecraft velocity is included as an input and ram and wake effects are modelled. One or two Maxwellian components may be used to define the ambient plasma. The electron population in POLAR is a superposition of power-law, Maxwellian, and Gaussian components. Once the surface currents have been found, POLAR calculates potentials and the equilibrium charging state in a similar way to NASCAP. The point of contact for the POLAR charging code is Air Force Research Laboratory, Hanscom Air Force Base, USA.

E.2.4 NASCAP-2K

The most recent NASCAP code, NASCAP-2K, is available free to US citizens only. This is a comprehensive code with realistic geometry. It combines the capabilities of NASCAP/GEO, NASCAP/LEO and POLAR. The code is not easily available outside the US due to export restrictions.

E.2.5 SPIS

SPIS (see Reference [31]) is a fully 3D particle-in-cell (PIC) that allows exact computation of the sheath structure and the current collected by spacecraft surfaces for very detailed geometries. Surface interactions including photoelectron emission, back-scattering, secondary electron emission and conduction are modelled. The source code is freely available from www.spis.org and a mailing list provides limited support.

E.2.6 MUSCAT

MUSCAT (see Reference [32]) is a fully 3D particle code that can be applied to spacecraft in LEO, PEO and GEO. Its algorithm is a combination of PIC and particle tracking. A parallel computation technique is used for fast computation. It has a JAVA-3D-based graphical user interface for 3D modelling of spacecraft geometry and output visualization. The surface interactions included in the NASCAP series and SPIS are modelled. A material property database is also included. The code is available commercially upon request from MUSCAT Space Engineering Co., Ltd., Japan.

E.2.7 Other surface charging codes

There are a number of other codes available to simulate surface charging. Two Russian codes ECO-M[33] and COULOMB[34] perform a very similar function to NASCAP, POLAR and NASCAP/LEO.

E.2.8 Environment Workbench

Environment Workbench (EWB) is an approximate, quick-look code that includes spacecraft charging in LEO. A variant of EWB is the official charging tool for the International Space Station (ISS). The point of contact for the code is Science Applications International Corporation, USA.

E.2.9 SPARCS

SPARCS is a code developed and used by Thales Alenia Space for simulating surface charging in the outer magnetosphere (GEO). This code computes the total current, due to all the primary and secondary current contributions, for each surface on a finite-element-type geometrical model of the spacecraft. Physical phenomena accounted for in the secondary current budget are electron photo-emission, back-scattering and secondary cascade emission, and secondary electron recollection. SPARCS uses a double Maxwellian environment for both ions and electrons. From these currents, the change in absolute potential of the spacecraft and in potential at each surface is calculated. Environmental conditions can be changed during computation for a simulation of an end-of-eclipse. SPARCS can be made available commercially upon request from Thales Alenia Space.

Annex F
(informative)

Derivation of theoretical surface flashover current

This annex presents an example of how to derive the theoretical flashover current based on Reference [35]. References [36] and [37] also give similar methods.

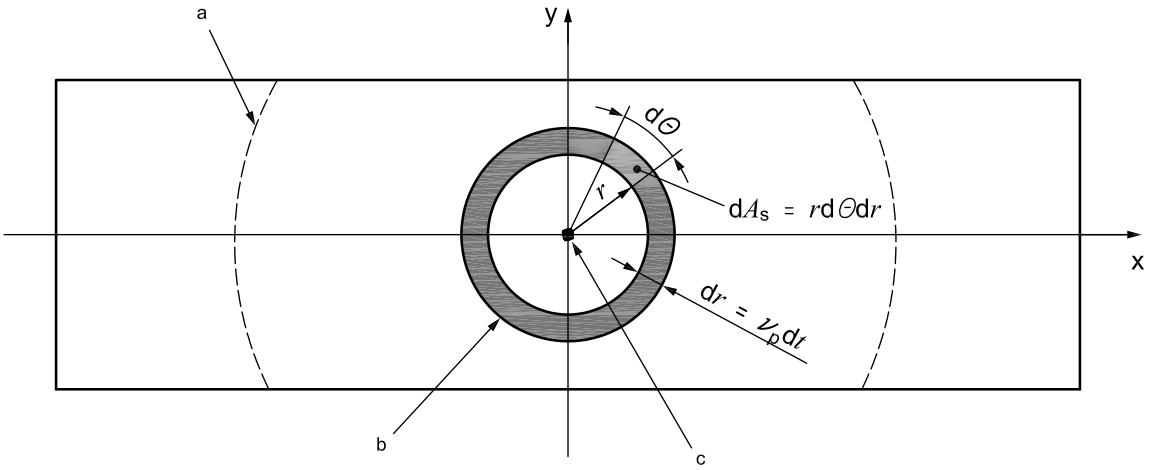

Key

A_S area of surface of plasma
r radius of plasma
t time
v_p velocity of plasma wavefront
θ angle

a Maximum propagation distance.
b Flashover plasma front.
c ESD inception point.

Figure F.1 — Model of surface flashover plasma propagation

Figure F.1 shows a surface flashover plasma propagation model. It is assumed that a ring shape of plasma propagates outward neutralizing charge stored on the coverglass. A current, dI, due to the charge stored in an area element, dA_S, is given by Equation F.1:

$$dI = \frac{dQ}{dt} = \frac{C_v dA_s \Delta V}{dt} = \frac{C_v r d\theta \cdot dr \Delta V}{dt} \quad \text{(F.1)}$$

where:

Q is the charge;

t is the time;

C_V is the capacitance per unit area of coverglass;

A_s is the area of surface of the plasma;

ΔV is the differential voltage of the coverglass before ESD inception;

r is the radius of the plasma;

θ is the angle.

The radius of the plasma wavefront increases at $v_p = dr/dt$. Equation F.1 shows that the stored charge is provided as soon as the flashover plasma reaches the coverglass. An instantaneous flashover current $I(t)$ is given by Equation F.2:

$$I(t) = \int_{\theta} C_v \Delta V \cdot v_p \cdot r \, d\theta \tag{F.2}$$

where the integral over the angle θ is carried out only for the angle where the plasma wavefront has not reached the edge of the solar panel. Assuming that a flashover propagates over a solar paddle whose lateral dimension is 2,4 m with a constant velocity of v_p = 10 km/s and that the coverglass with C_v = 200 nF/m^2 is charged to ΔV = 1 000 V, one gets the flashover current waveform shown in Figure F.2, where the maximum propagation distance of 2 m radius is assumed. When the flashover plasma front reaches the edge of the solar paddle (1,2 m from the ESD inception point), there is a peak in the current.

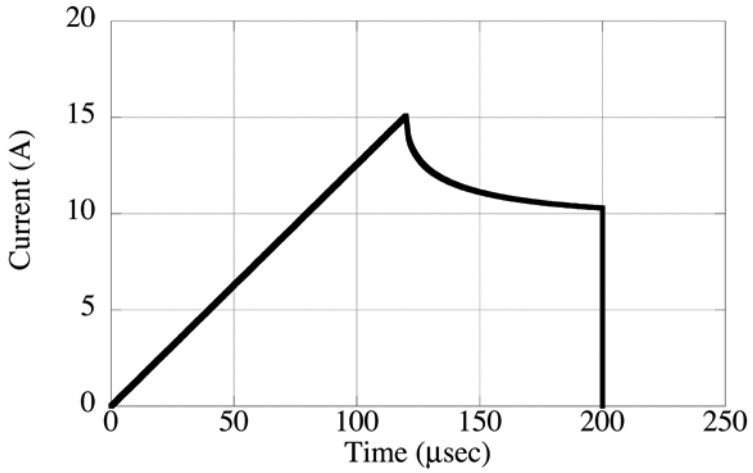

NOTE Conditions: C_v = 200 nF/m^2; ΔV = 1 000 V; v_p = 10 km/s; maximum propagation distance of 2 m.

Figure F.2 — Example of surface flashover current calculated by Equations F.1 and F.2

Annex G
(normative)

External circuit of secondary arc test

Figure G.1 provides a schematic illustration of a recommended circuit layout for a secondary arc test representing IPG.

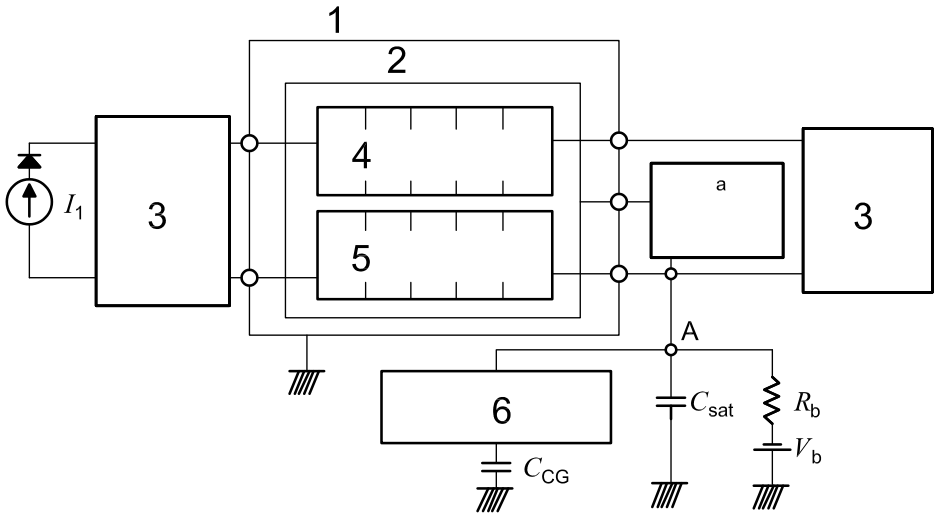

Key

1	vacuum chamber	C_{CG}	capacitor representing capacitance between exterior insulator surface and spacecraft ground
2	substrate	C_{sat}	capacitor representing capacitance between satellite body and ambient plasma
3	solar array string simulator	I_1	power supply representing power generated by the solar array
4	HOT string	R_b	resistance
5	RTN string	V_b	power supply representing charging potential of spacecraft body
6	pulse-forming circuit		

[a] Ground resistance, if any.

Figure G.1 — Recommended circuit layout of a secondary arc test representing IPG

The HOT string represents solar cells at a positive potential with respect to the spacecraft chassis and the RTN (return) string represents solar cells close to the spacecraft chassis. The power supply V_b represents the charging potential of the spacecraft body. The resistance R_b should be inserted to isolate the power supply from the circuit during the transient. The easiest way to detect the occurrence of a primary discharge is to monitor the voltage between point A and the ground. The vacuum chamber serves as the circuit ground.

The circuit has two capacitors that simulate the energy source in primary discharge. The capacitor C_{sat} represents the capacitance between the satellite body and the ambient plasma. As this is usually in the order of 100 pF to 1 000 pF, it may be substituted by the floating capacitance between the circuit and ground. The wire harness alone often has a capacitance greater than 100 pF. The capacitor C_{CG} represents the capacitance between the exterior insulator surface and the spacecraft ground that provides the electrostatic energy as the surface flashover current. Since C_{CG} is charged by the power supply V_b, it is necessary to adjust the value of C_{CG} so that the current provided by C_{CG} is representative of the surface flashover current in orbit. The fact that the surface flashover propagates with a finite speed shall be taken into account. A pulse-forming circuit, such as the insertion of inductance and resistance, should be used to delay the energy injection from

C_{CG}. Dividing C_{CG} into small parallel capacitances that are connected individually in series with time-delayed switches also provides a representative energy comparable with primary discharge. If no pulse-forming circuit is used, the energy may be released more quickly, which can cause more severe effects. Care shall be taken to make sure ringing or other side effects that are not representative of the situation in orbit do not occur. Though the wire harness shall be representative of a flight solar panel, the cable length should be minimized, or co-axial cable should be used, to reduce unwanted excessive inductance.

The solar array string simulator on the right of Figure G.1 may be opened, short-circuited or inserted with resistance. The string simulator may include all or some of the spacecraft internal circuit elements, e.g. blocking diodes, a bypass capacitance, load resistance, shunting electronics and so on. Care shall be taken to ensure that the following requirements are met.

a) All the available current from at least a string of the solar array circuit, i.e. the short-circuit current, shall become available to a secondary arc once the resistance of the secondary arc plasma drops to a significantly low level. A diode switch as described in References [12] and [38] should be used.

b) The voltage between the HOT and RTN strings shall not increase too much due to the surge voltage induced by the primary discharge current to the HOT string. If the load simulator is open or has only resistive components, the passage of the primary discharge current shall produce a high voltage drop, especially when a large C_{CG} is used. A large capacitance (approximately 10 mF or more) should be inserted in the load simulator representing the bus capacitance, providing a path for the high-frequency primary discharge current and producing a smaller voltage drop.

The power supply I_1 represents the power generated by the solar array. A diode should be inserted to protect the power supply from the primary discharge hitting the HOT string. The power supply shall be capable of reproducing the dynamic response of the array to transient short circuits such as limited overshoot current and fast recovery to the steady state. The solar array string simulator may include string capacitance and face-sheet capacitance. The string capacitance is the capacitance associated with the differential mode between the two ends of the string. The face-sheet capacitance is the capacitance between the solar cells and the conductive substrate through the adhesive and polymer face-sheet. See References [12] and [38] for details of the derivation of these capacitances. If the blocking diodes do not isolate every solar array string circuit, all of the solar array strings grouped by each blocking diode shall be considered to give power to a secondary arc. Then, either the power supply I_1 shall provide the total power or the solar array string simulator shall include power supplies to represent contributions from the non-arced strings. See References [12] and [38] for details.

Specific examples of the circuit diagrams that are used in France, Japan and the US are shown in Figures G.2, G.3 and G.4 respectively.

There is also a method to simulate flashover propagation with a large sample of dielectric material charged inside the chamber at the same time as the test coupon. See References [40] and [41].

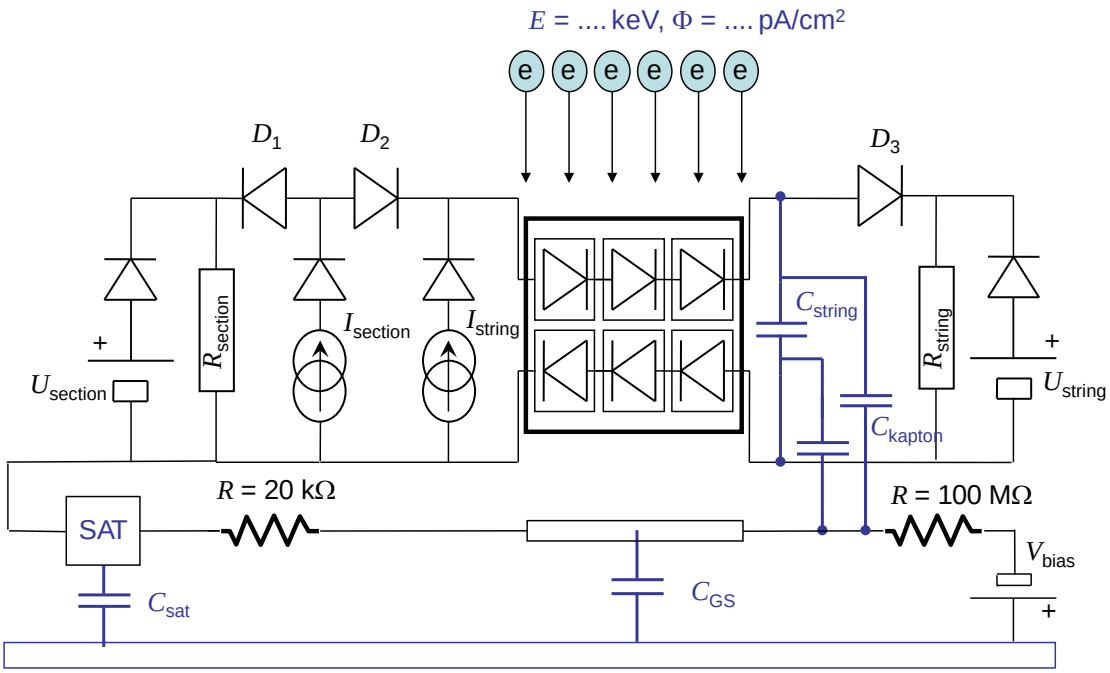

Key

SAT	satellite body
C_{GS}	capacitor representing capacitance between solar panel structure and ambient plasma
C_{kapton}	capacitor representing capacitance underneath the cells through the Kapton layer
C_{sat}	capacitor representing capacitance between satellite body and ambient plasma
C_{string}	capacitor representing capacitance of solar array string
D_1	fast switching diode
D_2	fast switching diode
D_3	fast switching diode
$I_{section}$	current of a solar array section
I_{string}	current of a solar array string
R	resistance
$R_{section}$	$U_{section}/I_{section}$, resistance needed to get the right voltage and current in the loop simulating the solar panels section
R_{string}	U_{string}/I_{string}, resistance needed to get the right voltage and current across the solar cells simulating the solar array string under arcing test
V_{bias}	power supply representing the charging potential of the spacecraft body
$U_{section}$	voltage of a solar array section
U_{string}	voltage of a solar array string

Figure G.2 — Example of the circuit layout for a secondary arc test representing IPG — France[38]
Courtesy of D. Payan

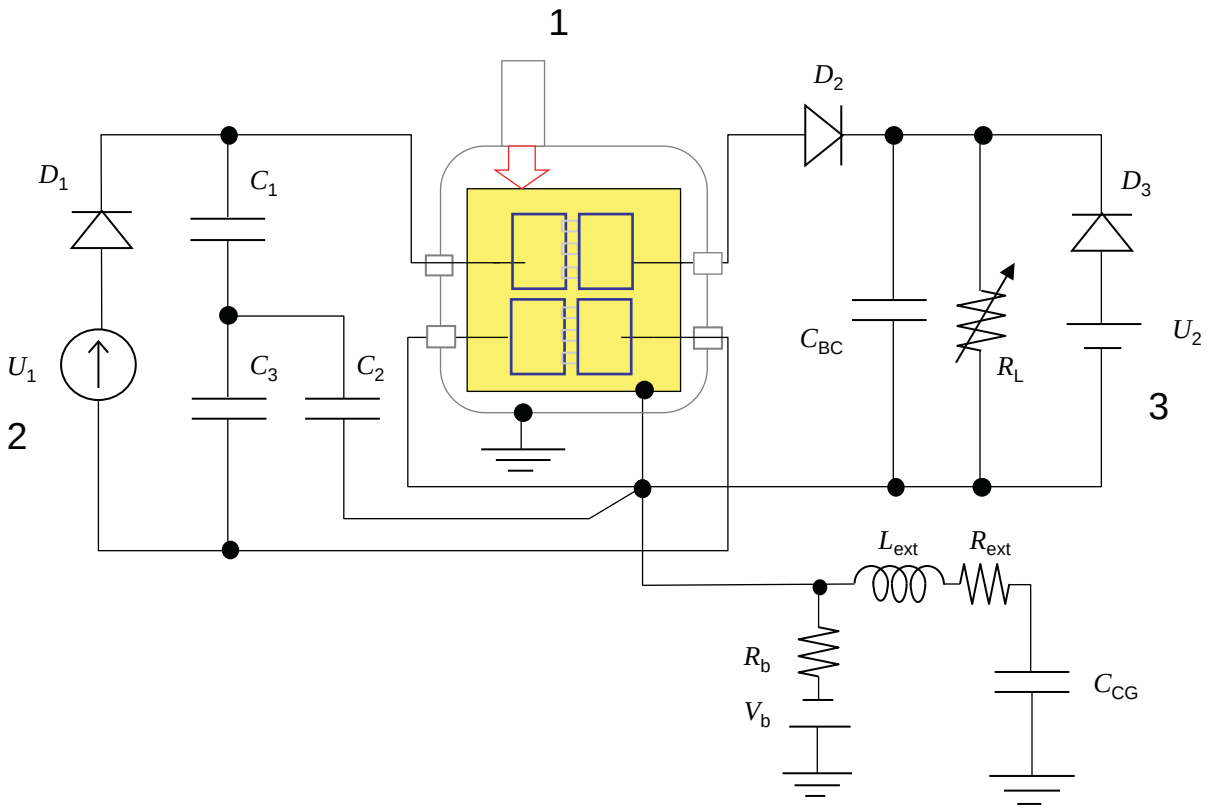

Key

1	electron beam or plasma source
2	CC source
3	CV source
C_1	capacitor representing the capacitance of the solar array string and the capacitance underneath the cells through the Kapton layer
C_2	capacitor representing the capacitance of the solar array string and the capacitance underneath the cells through the Kapton layer
C_3	capacitor representing the capacitance of the solar array string and the capacitance underneath the cells through the Kapton layer
C_{BC}	bypass capacitance
C_{CG}	capacitance between exterior insulator surface and spacecraft ground
D_1	fast switching diode
D_2	fast switching diode
D_3	fast switching diode
L_{ext}	inductance to form the pulse current shape
R_b	resistance
R_{ext}	resistance to form the pulse current shape
R_L	resistance to adjust the voltage between two strings under test
U_1	constant current source
U_2	constant voltage source
V_b	power supply representing charging potential of spacecraft body

Figure G.3 — Example of the circuit layout for a secondary arc test representing IPG — Japan[39] 3)

3) Reprinted with permission from AIAA.

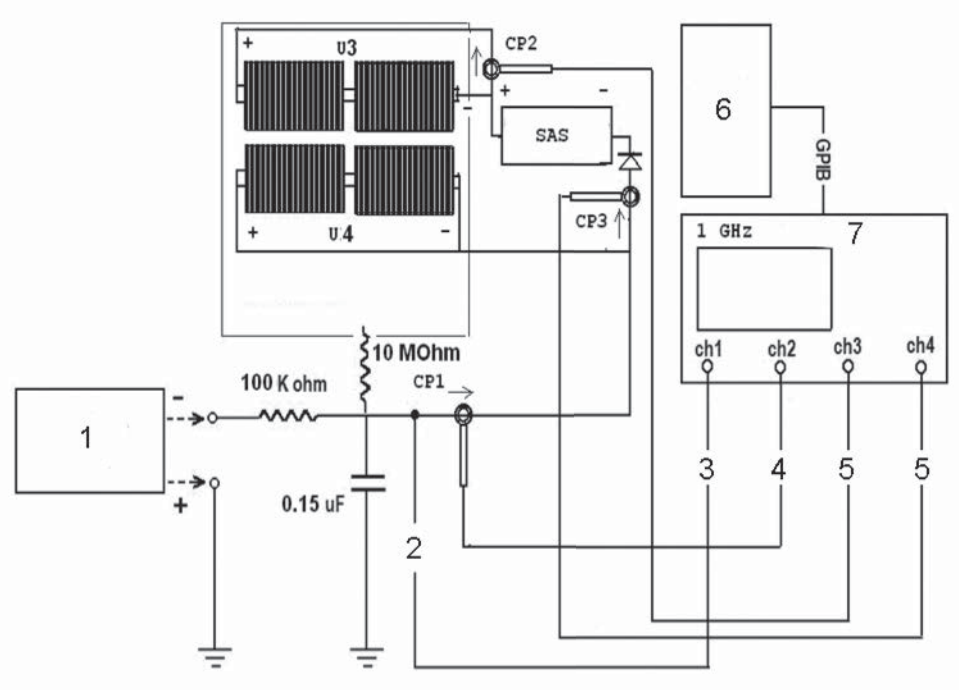

Key

1 0-1kV bias supply
2 voltage probe
3 voltage waveform (voltage WFM)
4 trigger pulse (trig. pulse)
5 current waveform (current WFM)
6 computer
7 oscilloscope

SAS solar array simulator
GPIB general purpose interface bus
CP1 current probe
CP2 current probe
CP3 current probe
U3 string
U4 string

Figure G.4 — Example of the circuit layout for a secondary arc test representing IPG — USA
© 2008 IEEE. Reprinted with permission from Reference [40]

Annex H
(informative)

Solar cell I-V characteristics measurement

The I-V characteristics should be measured under illumination at the same facility before and after the test because the relative change in the electrical performance is more important than the absolute performance value. The illuminated I-V curve measurement need not be carried out at the same location as the ESD/PI tests.

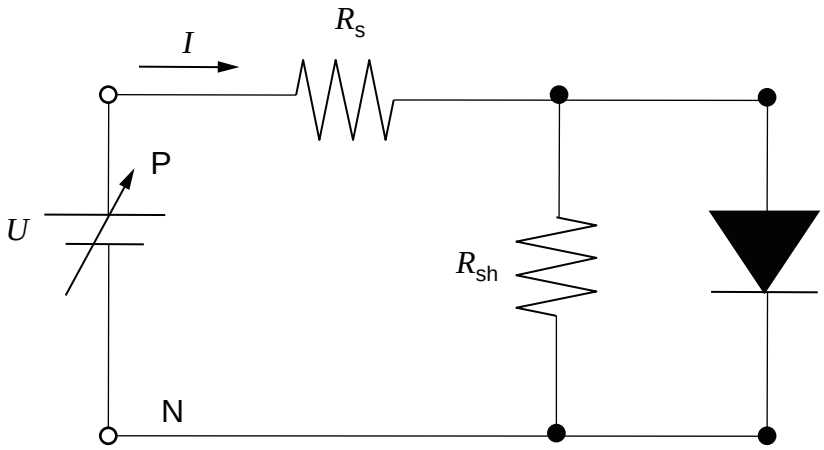

Figure H.1 — Equivalent circuit of a solar cell in dark conditions with an external DC power supply

It is useful to measure the dark current in situ to monitor the performance degradation. Figure H.1 illustrates the equivalent circuit of a solar cell in dark conditions. It consists of a diode, parallel shunting resistance, R_{sh}, and series resistance, R_s. The relationship between the current I and the voltage U applied by the external DC power supply is given by Equation H.1:

$$I = I_0 \left\{ \exp\left(\frac{q\left(U - R_s I\right)}{nkT} \right) - 1 \right\} + \frac{U - R_s I}{R_{sh}} \qquad \text{(H.1)}$$

where

I_0 is the reverse saturation-current density, in amperes per square metre (A/m^2);

T is the temperature, in kelvins (K);

k is the Boltzmann constant;

n is the diode constant;

q is the elementary charge;

R_{sh} is the parallel shunting resistance;

R_s is the series resistance.

When a solar cell degrades due to ESD, the degradation appears as a decrease in parallel resistance, increase in series resistance, or a change in diode properties I_0 and n. In many cases, the decrease of the shunt resistance is the most notable and it can be found easily by plotting the dark I-V data in a semi-logarithmic plot as shown in Figure H.2. In this example, as R_{sh} is too low, even if the cell is illuminated, most of the photo-generated power leaks to R_{sh} instead of going to the load.

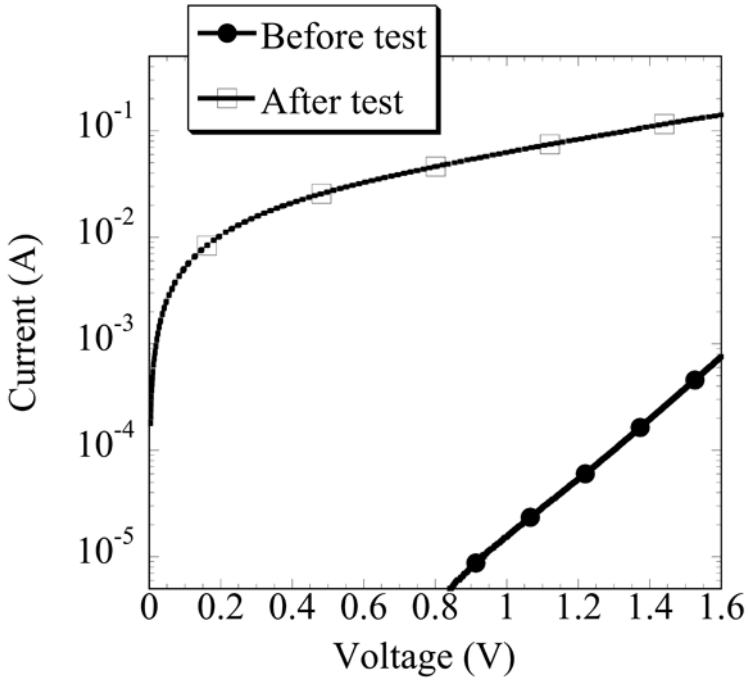

Figure H.2 — Example of the dark I-V characteristics of a solar cell before and after testing with an R_{sh} decrease

Annex I
(informative)

Secondary arc statistics

This annex provides an example, based on Reference [4], of deriving secondary arc statistics . Table I.1 gives the test results relating to a gap of a 2 x 2 solar array coupon. The table lists the voltage across the active gap, the string current, the total duration of the test, the number of arcs and the statistics on temporary sustained arc (TSA) duration, with the minimum, average, maximum and standard deviation.

In this example, a secondary arc lasting longer than 2 µs after the end of the primary discharge pulse was considered TSA. This criterion was applied to avoid the oscillatory noise associated at the end of the primary discharge pulse. The criterion of 2 µs may vary from laboratory to laboratory. On the basis of these results, the transition probability from a primary discharge to a secondary arc is derived as 170/290 = 0,586.

Table I.1 — Example of test result of secondary arc characterization test[4] 4)

U_{ST} (V)	I_{ST} (A)	Test duration (min)	Number of arcs					TSA duration (µs)			
			Total on test coupon	At active gap only				Min.	Avg	Max.	Std
				Total	PA	NSA	TSA				
70	1,0	174	294	290	92	28	170	2,2	31,8	685[a]	72,7

[a] Measurement taken over the range of the oscilloscope setting.

NOTE U_{ST} is string voltage and I_{ST} is string current.

Figure I.1 shows the positions of all 170 TSA listed in Table I.1. The ESD positions were extracted from the optical flash associated with each arc by processing the video image. In this example, the points located on the coverglass indicate that the flash associated with TSA was too bright to identify its location precisely.

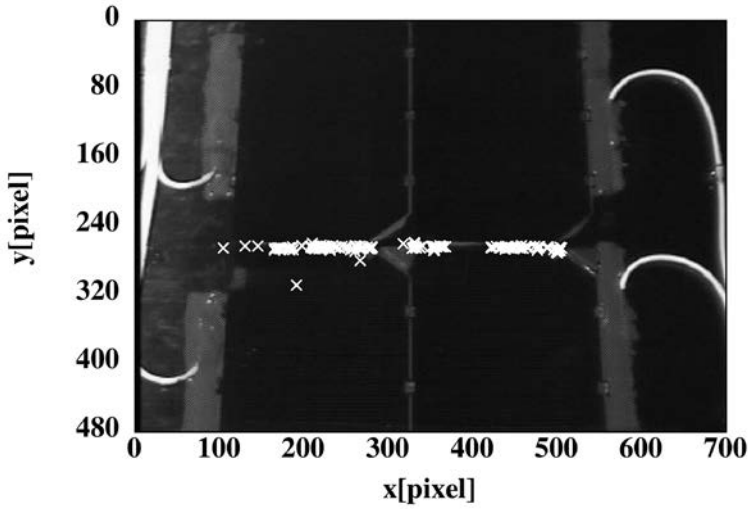

Figure I.1 — Positions of all TSA identified by a computer[4] 5)

4) Reprinted with permission from AIAA.

5) Reprinted with permission from AIAA.

Next, the distribution of TSA duration is plotted. The fraction of the 170 TSA events with a duration longer than t_{arc} is calculated. The fraction calculated in this way is equal to the probability, $P(t_{arc})$, of the arc having a duration longer than t_{arc}. The probability reaches unity at t_{arc} = 2 µs, that is, P(2 µs) = 1, because the minimum duration for TSA was set at 2 µs in this example. Figure I.2 shows the probability calculated from all of the 170 TSA events.

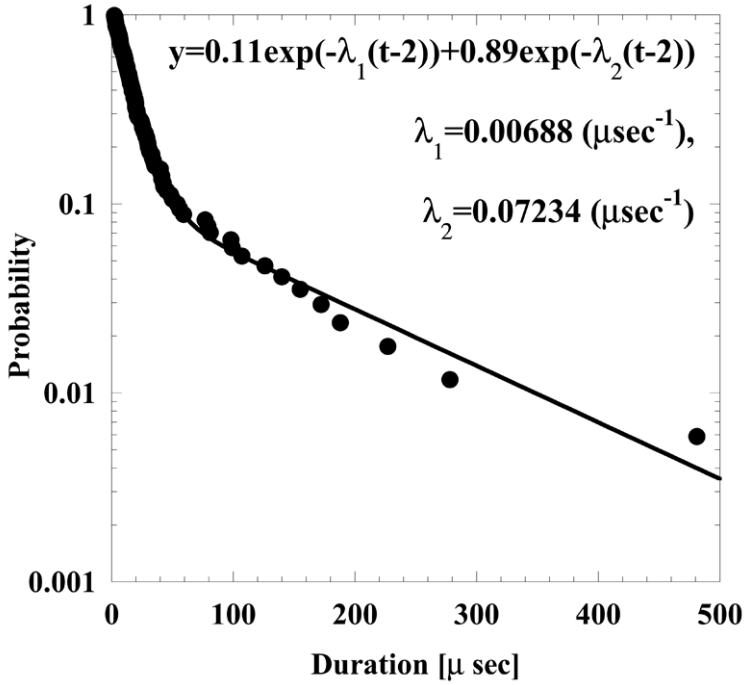

Figure I.2 — Probability distribution of TSA duration for all TSAs observed in the active gap[4] 6)

The data in Figure I.2 suggests that there are two straight lines in the logarithmic plot. Equation (I.1) fits the data points well:

$$P(t_{arc}) = P_1 \exp\{-\lambda_1(t - t_{arc})\} + (1 - P_1)\exp\{-\lambda_2(t - t_{arc})\} \quad \text{(I.1)}$$

with P_1 = 0,11, λ_1 = 0,006 88, λ_2 = 0,072 34. Equation (I.1) indicates that TSA duration is modelled by a combination of two Poisson distributions.

The value χ^2 is calculated to check how appropriately the probability distribution given by Equation (I.1) represents the data. The duration is divided into several bins and the width of each bin is adjusted so that each is expected to contain the same number. Then, χ^2 is given by Equation (I.2):

$$\chi^2 = \sum_1^j \frac{(y_i - nP_i)^2}{nP_i} \quad \text{(I.2)}$$

where

j is the number of bins;

P_i is the probability that an event occurs in the *i*-th bin;

n is the number of trials.

6) Reprinted with permission from AIAA.

In this case, n is the number of items of data. The degree of freedom is $(k - 4)$ for the present case, because the total number of items of data, P_1 and two lambdas are already assumed. The value of χ^2 calculated in accordance with Equation (I.1) varies depending on the expected value per bin. If the expected number per bin is taken to be approximately 10, the value of χ^2 is 3,916 2, in accordance with Table I.2 (sum the numbers in column 6). From a table of χ^2 distribution, with 13 degrees of freedom, the hypothesis cannot be denied that the duration follows the distribution given by Equation (I.2) with more than 98,6 % significance.

Table I.2 — χ^2 test of probability distribution given by Equation (I.2)

Bin No.	Range of bin (µs)		y_i	nP_i	$\frac{(y_i - nP_i)^2}{nP_i}$
	from	to			
1	2,0	3,0	12	10,69	0,160 53
2	3,0	4,1	11	10,91	0,000 74
3	4,1	5,2	9	10,08	0,115 71
4	5,2	6,4	10	10,13	0,001 67
5	6,4	7,7	12	10,04	0,382 63
6	7,7	9,2	7	10,49	1,161 12
7	9,2	10,8	9	10,02	0,103 83
8	10,8	12,7	11	10,51	0,022 84
9	12,7	14,8	11	10,08	0,083 97
10	14,8	17,3	11	10,21	0,061 13
11	17,3	20,3	13	10,10	0,832 67
12	20,3	24,1	7	10,10	0,951 49
13	24,1	29,3	10	10,15	0,002 22
14	29,3	37,3	10	10,06	0,000 36
15	37,3	54,5	10	10,02	0,000 04
16	54,5	154,5	10	9,871	0,001 69

Annex J
(informative)

Solar array back surface test

Although the scope of this International Standard is surface discharge and plasma interaction on the solar array front surface, the possibility of ESD and plasma interaction on the solar array back surface cannot be excluded. Reference [19] describes an example of an ESD test on a solar array back surface.

As there is no solar cell on the back surface, secondary arcs and power leakage are the major concerns. A solar array back surface often has exposed metallic parts such as diodes, connectors, hold-down, etc. If the metallic parts are adjacent to other parts with a different voltage, a primary ESD on the solar array back surface can lead to a secondary arc between the two parts and a subsequent permanent short circuit. The metallic parts may attract electrons from the surrounding plasma if their potential with respect to the plasma is high, resulting in power leakage to the plasma.

Apart from the test coupon, the same test facility and procedure as used for the test on the front surface can be applied to the test on the back surface. The test coupon should be made in the same manner as the flight solar panel, including the substrate. All the features of the flight panel such as diode boards, connectors, etc. should be included. The test flow for a secondary arc is the same as for the front surface. First, the ESD inception threshold should be measured as described in Clause 6, using a charging method representative of the orbital condition. Many charging analysis software programs are capable of calculating the back surface differential charging at the same time as they calculate the front surface charging. Therefore, it is possible to estimate the number of ESD events in orbit as described in Annex D. The secondary arc test on the back surface can be performed in the same manner as given in 7.2 and 7.5, using the flight-representative back surface coupon. The same external circuit as that described in 7.3 and Annex G can be used, although care should be taken to derive the correct value of the external capacitance, because the flashover extension is now over the insulator on the back surface.

The power leakage test on the back surface can be carried out in the same manner as given in 8.3, except for the test coupon. The same test coupon as was used for the back surface ESD test can be used for the plasma leakage test. As most spacecraft use negative grounding of the solar array circuit, power leakage to the solar panel substrate is not a concern. Exposed metallic parts with the same potential as the positive end of the solar array circuit, such as blocking diodes, have the highest risk of serious power leakage. Those parts should be included in the test coupon.

Bibliography

[1] VAYNER, B., GALOFARO, J. and FERGUSON, D., Interactions of High-Voltage Solar Arrays with Their Plasma Environment: Ground Tests, *Journal of Spacecraft and Rockets*, Vol. 41, No. 6, 2004, pp. 1031-1051

[2] FERGUSON, D.C., *The voltage threshold for arcing for solar cells in LEO: Flight and ground test results*, NASA-TM-87259 or AIAA Paper 86-0362, 1986

[3] MASHIDORI, H., IWASA, M., WADA, A., NITTA, K., NOMURA, M., TOYODA, K., Preliminary ESD Ground Tests on Meter-Class Solar Panels in Simulated GEO Environments, *4th Space Environment Symposium*, Tokyo, Japan, 22-23 January 2008

[4] CHO, M., KITAMURA, K., OSE, T., MASUI, H., TOYODA, K., Statistical Number of Primary Discharges Required for Solar Array Secondary Arc Tests, *Journal of Spacecraft and Rockets*, Vol. 46, No. 2, 2009, pp. 438-448

[5] CHO, M., Ionosphere Ionization Effects on Sheath Structure around a High Voltage Spacecraft, *J. Spacecraft and Rockets*, Vol. 32, No. 6, 1995, pp. 1018-1026

[6] COOKE, D.L. and KATZ, I., Ionization-induced instability in an electron-collecting sheath, *J. Spacecraft and Rockets*, Vol. 25, No. 2, 1988, pp. 132-138

[7] ISO/TS 16457, *Space systems — Space environment (natural and artificial) — The Earth's ionosphere model: international reference ionosphere (IRI) model and extensions to the plasmasphere*

[8] http://ccmc.gsfc.nasa.gov/modelweb/

[9] FERGUSON, D.C. and HILLARD, G.B., *Low Earth Orbit Spacecraft Charging Design Guidelines*, NASA/TP-2003-212287

[10] NASA-STD-4005, *Low Earth Orbit Spacecraft Charging Design Standard*

[11] NASA-HDBK-4006, *Low Earth Orbit Spacecraft Charging Design Handbook*

[12] ECSS-E-ST-20-06C, *Space Engineering — Spacecraft Charging*, 2008

[13] PURVIS, C.K., GARRETT H.B., WHITTLESEY, A.C. and STEVENS J.N., *Design Guidelines for Assessing and Controlling Spacecraft Charging Effects*, NASA Technical Paper 2361, 1984

[14] PAYAN, D., SEVERIN, F., CATANI, J.P., ROUSSEL, J.F., REULET, R., SARRAIL, D., Electrostatic Discharges on Solar Arrays. Physical Model of Inverted Potential Gradient Electrostatic Discharge, *7th Spacecraft Charging Technology Conference*, ESA/ESTEC Noordwijk, The Netherlands, 23-27 April 2001. Available at: http://dev.spis.org/projects/spine/home/tools/sctc

[15] HASTINGS, D.E., CHO, M. and KUNINAKA, H., The Arcing Rate for a High Voltage Solar Array: Theory, Experiment and Predictions, *J. Spacecraft and Rockets*, Vol. 29, 1992, pp. 538-554

[16] HASTINGS, D.E., WYLE, G. and KAUFMAN, D., Threshold Voltage for Arcing on Negatively Biased Solar Arrays, *J. Spacecraft and Rockets*, Vol. 27, 1990, pp. 539-544

[17] CHO, M., RAMASAMY, R., MATSUMOTO, T., TOYODA, K., NOZAKI, Y., TAKAHASHI, M., Laboratory Tests on 110-Volt Solar Arrays in Simulated Geosynchronous Orbit Environment, *J. Spacecraft and Rockets*, Vol. 40, No. 2, 2003, pp. 211-220

[18] CHO, M. and GOKA, T., Japanese practices of solar array ESD ground tests, *9th Spacecraft Charging Technology Conference*, Tsukuba, Japan, April 2005, JAXA SP-05-001E. Available at: http://repository.tksc.jaxa.jp/dr/prc/japan/contents/AA0049206046/49206046.pdf

[19] CHO, M., KIM, J.-H., HOSODA, S., NOZAKI, Y., MIURA, T., IWATA, T., Electrostatic Discharge Ground Test of a Polar Orbit Satellite Solar Panel, *IEEE Transaction on Plasma Science*, Vol. 34, No. 5, 2006, pp. 2011-2030

[20] BERTHOU, C., BOULANGER, B., LEVY, L., Plasma ESD Qualification Test Procedure of Alcatel Alenia Space Solar Array, *IEEE Transaction on Plasma Science*, Vol. 34, No. 5, 2006, pp. 2004-2010

[21] GAILLOT, L, FILLE, M-L., LEVY, L., Secondary arcs on solar array — Test results of emags 2, *9th Spacecraft Charging Technology Conference*, Tsukuba, Japan, April 2005, JAXA SP-05-001E. Available at: http://airex.tksc.jaxa.jp/pl/dr/AA0049206043/en

[22] FERGUSON, D.C., VAYNER, B.V., GALOFARO, J.T., HILLARD, G., VAUGHN, J., SCHNEIDER, T., NASA GRC and MSFC Space Plasma Arc Testing Procedures, *IEEE Transaction on Plasma Science*, Vol. 34, No. 5, 2006, pp. 1948-1958

[23] HOEBER, C.F., ROBERTSON, E.A., KATZ, I., DAVIS, V.A. and SNYDER, D.B., *Solar Array Augmented Electrostatic Discharge in GEO*, AIAA Paper 98-1401, 1998

[24] ECSS-ST-E10-04C, *Space engineering — Space Environment*, 2008

[25] CHO, M., KAWAKITA, S., NAKAMURA, S., TAKAHASHI, M., SATO, T. and NOZAKI, Y., Number of arcs estimated on solar array of a geostationary satellite, *Journal of Spacecraft and Rockets*, Vol. 42, No. 4, 2005, pp. 740-748

[26] http://cdaweb.gsfc.nasa.gov/

[27] http://sd-www.jhuapl.edu/Aurora/index.html

[28] http://cindispace.utdallas.edu/DMSP/

[29] KATZ I., CASSIDY, J.J., MANDELL, M.J., SCHNUELLE, G.W., STEEN, P.G. and ROCHE, J.C., The Capabilities of the NASA Charging Analyzer Program, in *Spacecraft Charging Technology –1978*, Ed. R.C. Finke and C.P. Pike, NASA CP-2071/AFGL TR-79-0082, ADA045459, p. 101, 1979

[30] LILLEY, J.R., COOKE, D.L., JONGEWARD, G.A. and KATZ, I., *POLAR User's Manual*, AFGL-TR-85-0246

[31] FOREST, J., ELIASSON, L. and HILGERS, A., A New Spacecraft Plasma Interactions Simulation Software, PicUp3D/SPIS, *Proc. 7th Spacecraft Charging Technology Conf.*, 2001, pp. 515-520. Available at: http://dev.spis.org/projects/spine/home/tools/sctc

[32] MURANAKA, T., HOSODA, S., KIM, J., HATTA, S., IKEDA, K., HMANAGA, T., CHO, M., USUI, H., UEDA, H.O., KOGA, K. and GOKA, T., Development of Multi-Utility Spacecraft Charging Analysis Tool (MUSCAT), *IEEE Transaction on Plasma Sciences*, Vol. 36, No. 5, 2008, pp. 2336-2349

[33] VASILYEV, Ju.V, DANILOV, V.V., DVORYASHIN, V.M., KRAMRENKO, A.M. and SOKOLV, V.S., Computer Modeling of Spacecraft Charging Using ECO-M, *Proc. International Conference of Problems of Spacecraft/Environment Interactions*, 15-19 June 1992, Novisibirsk, Russia, p. 187, 1993

[34] SOUBEYRAN, A., DROLSHAGEN, G., LEVY, L., MATUCCI, A., KENSEK, R.P., BETZ, G. and FEHRINGER RUDENHAUER, F.G., Deep Dielectric Charging Simulation New Guidelines, *IEEE proceedings of Radiation Effects Data Workshop*, IEEE, 21 July 1993, pp. 93-98

[35] MASUI, H., TOYODA, K. and CHO, M., Electrostatic Discharge Plasma Propagation Speed on Solar Panel in Simulated Geosynchronous Environment, *IEEE Transaction on Plasma Science*, Vol. 36, No. 5, 2008, pp. 2387-2394

[36] LEUNG, P., Plasma Phenomena Associated with Solar Array Discharges and their Role in Scaling Coupon Test Results to a Full Panel, AIAA 2002-0628, *40th Aerospace Sciences Meeting & Exhibit*, Reno, January 2002

[37] AMORIM, E., PAYAN, D., REULET, R. and SARRAIL, D., Electrostatic discharges on a 1 m^2 solar array coupon — Influence of the energy stored on coverglass on flashover current, *9th Spacecraft Charging Technology Conference*, Tsukuba, Japan, April 2005, JAXA SP-05-001E. Available at: http://repository.tksc.jaxa.jp/dr/prc/japan/contents/AA0049206042/49206042.pdf

[38] PAYAN, D., SCHWANDER, D. and CATANI, J.P., Risks of low voltage arcs sustained by the photovoltaic power of a satellite solar array during an electrostatic discharge. Solar Array Dynamic Simulator, *7th Spacecraft Charging Technology Conference*, April 2001. Available at: http://dev.spis.org/projects/spine/home/tools/sctc

[39] MASUI, H., KITAMURA, T., OKUMURA, T., TOYODA, K. and CHO, M., Laboratory Test Campaign for ISO Standardization of Solar Array ESD Test Methods, *AIAA 45th Aerospace Science Meeting*, 2007

[40] VAYNER, B., FERGUSON, D.C., GALOFARO, J. T., Emission Spectra of Arc Plasmas, *IEEE Transaction on Plasma Science*, Vol. 36, No. 5, 2008, pp. 2219-2227

[41] PAYAN, D., SCHWANDER, D., ROUSSEL, F., INGUIMBERT, V., SARRAIL, D., MATEO-VELEZ, J-C., CNES-ONERA Recommended Test Set-Up to Qualify Solar Array Design against Sustained Arc Triggered by an Electrostatic Discharge, *8th European Space Power Conference*, September 2008. Available at: www.congrex.nl/08a02/abstracts/317600.pdf

[42] PAYAN, D., ONERA/CNES Physical Flashover Simulator, *Proceedings of 6th Space Environment Symposium*, Kitakyushu, October 2009, JAXA SP-09-006

ICS 49.140

Price based on 44 pages